

***Bodo's** Power Systems®*

Electronics in Motion and Conversion

January 2021

Say Hello to the Future

First 750V SiC FETs



WELCOME TO THE HOUSE OF COMPETENCE

ENGINEERING

PRODUCTION

GvA SOLUTIONS

DISTRIBUTION



POWER

IS IN OUR NATURE!

Power is in our nature. Everyday we deliver full power for your success.

- ➡ **ENGINEERING:** Quick design-to-product using state-of-the-art technologies
- ➡ **PRODUCTION:** Extensive production experience with maximum flexibility
- ➡ **GvA SOLUTIONS:** Short time-to-market with innovative plug&play system solutions
- ➡ **DISTRIBUTION:** Vast product knowledge and consulting expertise

GvA Leistungselektronik GmbH

Boehringer Straße 10 - 12

D-68307 Mannheim

Phone +49 (0) 621/7 89 92-0

info@gva-leistungselektronik.de

www.gva-leistungselektronik.de



Power Electronics

Best Choice for High Current Carrying AC Application



5MPA FEATURES

- ✓ Low loss, dry film construction
- ✓ Operating temperature range: -55°C to +85°C
- ✓ Available off the shelf

Visit us online at www.ecicaps.com

Contact Us

North America: sales@ecicaps.com

Europe: sales@ecicaps.ie

CONTENT

Viewpoint	4	Capacitors	32-33
365 New Days, 365 New Chances!		Enabling High Temperature Operation of Optimized DC Link/Bus Test Kit	
Events	4	By M. A. Brubaker and E. D. Sawyer, Advanced Conversion and L. Schosseler, DuPont Teijin Films (DTF)	
News	6-12	Power Management	34-37
Product of the Month	14	Bidirectional Wireless EV Charging - Smart Grid Integration at Highest Comfort Level	
High Flux Titanium Series (GT Grade)		By Sri Vijay Vangapandu and Tobias Herrmann, Finepower	
Green Product of the Month	16	Design and Simulation	38-39
IGBT Module Contributes to Energy Saving in Railway Transportation		3D Bond Wire Modelling and Electro-Magnetic Simulation Accelerates IGBT Module Development	
Cover Story	18-22	By Raffael Schnell, SwissSEM Technologies AG and Samuel Hartmann, MFis GmbH	
750V Gen 4 SiC FETs Enable Higher Efficiency Power Designs		EMC	40-41
By Anup Bhalla, V.P. Engineering, United Silicon Carbide Inc.		GaN Transistor Eliminates EMC at Source	
Wide Bandgap	24-27	By Nigel Springett, Ing Büro Springett	
Layout Considerations for GaN Transistor Circuits		Technology	42-43
By Alex Lidow Ph.D., CEO and Co-founder, Efficient Power Conversion		Innovative Manufacturing Approach Reduces Costs and Optimizes Electrification Time to Market	
MOSFET	28-30	By Ermanno Faccin, Head of Powertrain & Electrical Drive Unit - Assembly & Test, Comau	
1200 V Discrete SiC MOSFETs in a Comparison with the HighSpeed 3 IGBTs for Servo-Drive Systems		New Products	44-48
By Blaž Klobučar and Dr. Zhihui Yuan, Infineon Technologies AG, Austria			

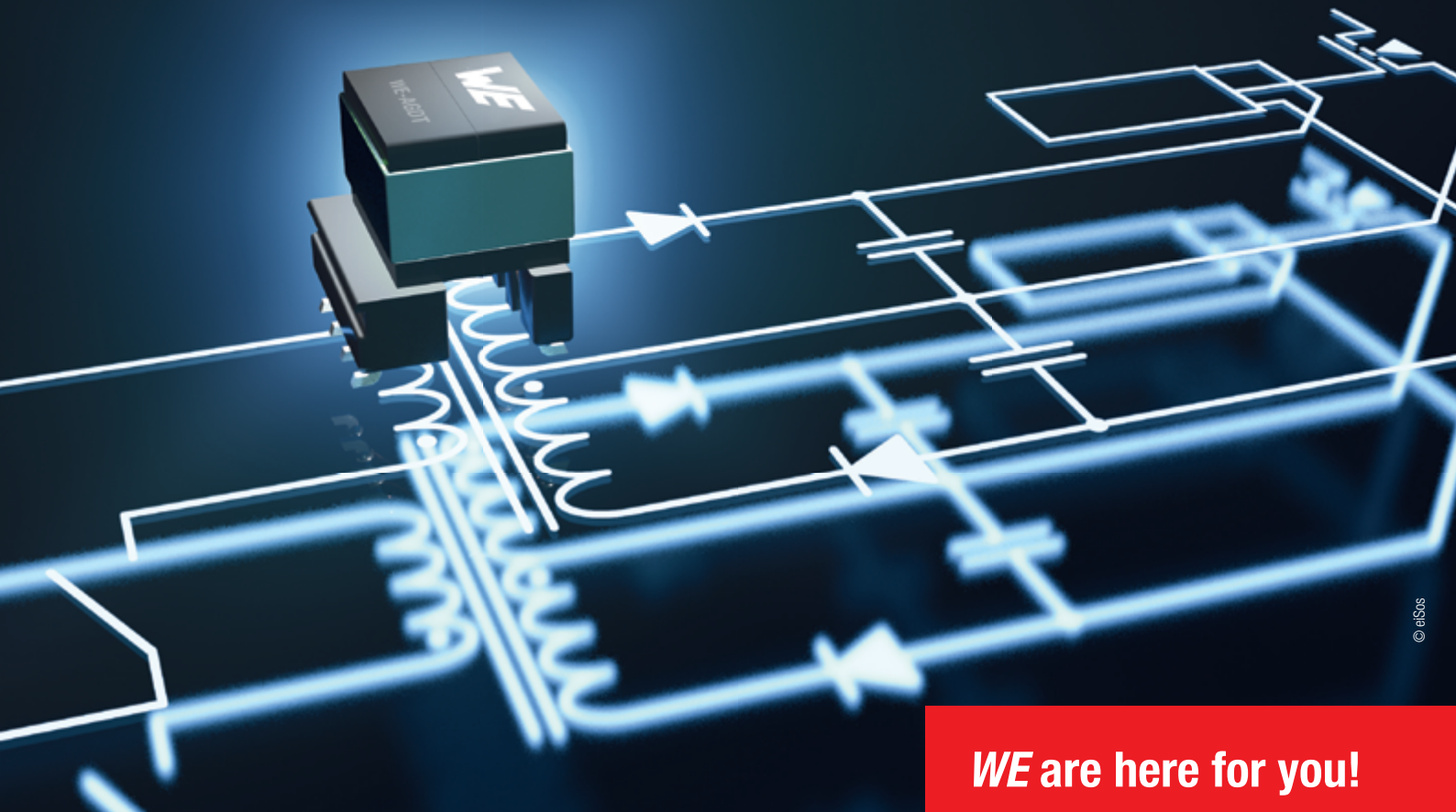


The Gallery



Drive hard. Drive safe.

WE-AGDT Gate Drive Transformer



© eISOS

WE are here for you!

Join our free webinars on
www.we-online.com/webinars

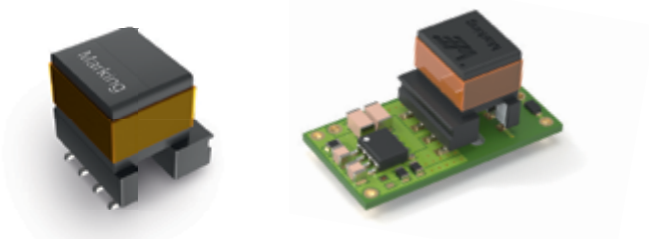
WE-AGDT

The WE-AGDT series from Würth Elektronik allows implementing discrete SiC gate driver designs easier than ever before. These standard parts are compact SMT transformers optimized for silicon carbide applications. With extremely low interwinding capacitance, the WE-AGDT helps to achieve higher Common Mode Transient Immunity (CMTI). The series is compliant with safety standards according to IEC62368-1 / IEC61558-2-16 in addition to AEC-Q200 qualification. Reference designs are available for each WE-AGDT transformer. The complete solution is compact and capable of fully automated assembly.

Products available from stock. Samples free of charge.

For further information, please visit: www.we-online.com/agdt

- Optimized for SiC gate driver supply
- Interwinding capacitance down to 6.8 pF
- CMTI over 100 kV/μs
- IEC62368-1 / IEC61558-2-16
- Up to 6 W power
- Unipolar & bipolar output
- Compact & lightweight



#ReadyForTheFuture

Bodo's Power Systems®

A Media

Katzbek 17a
D-24235 Laboe, Germany
Phone: +49 4343 42 17 90
Fax: +49 4343 42 17 89
info@bodospower.com
www.bodospower.com

Publisher

Bodo Arlt, Dipl.-Ing.
editor@bodospower.com

Editor

Holger Moscheik
Phone + 49 4343 428 5017
holger@bodospower.com

Editor China

Min Xu
Phone: +86 156 18860853
xumin@i2imedia.net

US Support

Cody Miller
Phone +1 208 429 6533
cody@eetech.com

Creative Direction & Production

Bianka Gehlert
b.gehlert@t-online.de

Free Subscription to qualified readers

Bodo's Power Systems
is available for the following
subscription charges:

Annual charge (12 issues)
is 150 € world wide

Single issue is 18 €
subscription@bodospower.com



Printing by:

Brühlsche Universitätsdruckerei GmbH
& Co KG; 35396 Gießen, Germany

A Media and Bodos Power Systems

assume and hereby disclaim any
liability to any person for any loss or
damage by errors or omissions in the
material contained herein regardless
of whether such errors result from
negligence accident or any other cause
whatsoever.



www.bodospower.com

Events

NEPCON 2021

Tokyo Big Sight, Japan January 20-22
www.nepconjapan.jp/en

India Electronics Week 2021

Bengaluru, India February 3-5
www.indiaelectronicsweek.com

IPC APEX 2021

Online March 8-12
www.ipcapexexpo.org

embedded world 2021

Online March 1-5
www.embedded-world.de

365 New Days, 365 New Chances!

2020 is finally over and it is surely not going to be missed. This pandemic has caused a lot of sorrow and pain. It brought, and still brings, drastic changes to all our business and private lives and has changed the way that we interact with our families, friends, and colleagues. In early 2020 it was suddenly wrong to meet in person, whether for business or friendship. What a surprise it was when the first events had to be cancelled. Today, we know better - we were lucky that we did not meet in New Orleans or Nuremberg - strolling through crowded halls and having fun in the bars at night.

Bodo and I want to say a big Thank You to everyone who helped to make the virtual Wide Bandgap event early December what it was: a total success. Thank you to the sponsors for their support, to all the presenters who contributed their presentations and joined the live-sessions and to the audience for submitting their questions. And last but not least to our partners at AspenCore for taking care of all the administrative organization. If you missed the event, don't worry. All the presentations and the live sessions are available on demand on our website, just go to the WBG section and enjoy. It's a free and easily accessible collection of videos, just perfect for cold, dark January evenings. You also can send any questions to us direct and we will be happy to forward these to the experts.

As we did last year, instead of sending Christmas gifts, we have decided to donate to UNICEF. It feels right to support this welfare organization, which has been fighting for the wellbeing of children for over 70 years



now. While we are so focused on COVID, we should also keep in mind that many children still face health and poverty problems. For instance: in many areas of our world, fresh and clean water still does not come out of the wall!

Bodo's magazine is delivered by postal service to all places in the world. It is the only magazine that spreads technical information on power electronics globally. We have EETech as a partner serving North America efficiently. If you are using any kind of tablet or smart phone, you will find all our content on the website www.eepower.com. If you speak the language, or just want to have a look, don't miss our Chinese version: www.bodospowerchina.com

My Green Power Tip for the Month:

In the past, Coffee-filters, were compostable. Just recently, convenient and compostable capsules and pods are becoming available. For the environment, we should choose these!

Happy New Year from Bodo & Team



The smarter route to Electric Vehicle metering



DCBM Series

Smart and compact, the Direct Current Billing Meter (DCBM) gives charging station providers the ability to deliver a 'gas station' like experience, using an LCD display to show real time measurements, energy, alarms and legal data.

An excellent solution for retrofit and new DC Fast charging stations from 25 to 400 kW, the DCBM uses industry standard data protocols. The result is secure, authentic billing, easy connectivity to Cloud services and a faster certification process.

www.lem.com

- 400 A - 600 A maximum current
- 1000 V nominal voltage
- Class B accuracy
- Billing Meter in compliance with VDE-AR-E-2418-3-100
- Ethernet communications supporting the HTTPS/REST protocol
- Signed billing data sets according to the S.A.F.E OCMF

LEM

Life Energy Motion

EMV 2021 to be Held Digitally

Due to the pandemic and its effects, the EMV trade fair and parallel workshops are to take place digitally. The event is designed to once again give the EMC community a platform for exchange. Preparations



for the online solution are already underway. "We assume that even in the spring of 2021, travel restrictions and further limitations can still be expected," explains Petra Haarburger, President of the event organizer Mesago Messe Frankfurt. "We are delighted to be able to offer the international EMC community a digital alternative. Due to the early switch to an online edition, we are glad to provide exhibitors, speakers and all other attendees time to plan their participation."

As with the on-site event, the focus of the digital platform is on a practice-oriented exchange of knowledge and networking. Participants can use the chat and video call function, as well as discussion features and product presentations, to exchange information in a targeted manner. The matchmaking feature, based on areas of interests, offerings, and many other aspects, supports the community in quickly finding the right partner. "For the international EMC community in industry and science, this opens up new opportunities for efficient and sustainable networking," Petra Haarburger emphasizes.

www.e-emc.com

German Branch Becomes CharIN-Member

Mitsubishi Electric Europe B.V. German Branch is pleased to announce its acceptance as a member of the Charging Interface Initiative e. V. (CharIN). From the perspective of a manufacturer covering the supply of Power Semiconductors for a broad range of applications, Mitsubishi Electric Europe B.V. is glad to be able to contribute to the existing broad base of experts from different industries in CharIN to support the definitions of the requirements of combined charging systems and the future developments. Mitsubishi Electric is a leading manufacturer of Power Semiconductors as key parts of the control systems of electric power, in e-mobility as well as in renewable energies, energy storage, power transmission and distribution, railway technology and others. Mitsubishi Electric pioneered the mass production of power modules for hybrid vehicles in 1997 and is today a supplier of power semiconductors to the various categories of xEV. In industrial applications related to e-mobility, Mitsubishi Electric supplies power devices to manufactures of charging stations to ensure efficient High Power DC charging. The environmental statement of the



Mitsubishi Electric Group "Eco Changes" expresses the ambition to work together with our partners on technology leading to CO2 reduction to globally change the environment for the better.

www.mitsubishichips.eu

Continental "Supplier of the Year 2019 Award"

The Continental Automotive Group honors ROHM Semiconductor with the "Supplier of the Year 2019 Award" in the category "Discrete Semiconductors" for particularly outstanding performance. Since 2008, Continental conducts an annual broad-based analysis to identify exceptional contributions in customer satisfaction and at all levels of quality, technology, commitment, costs and purchasing conditions. This is the fifth time within the last ten years that ROHM has received this prestigious award. This year, the award was presented in a virtual ceremony. "We are pleased to honor ROHM Semiconductor's commitment with the Supplier of the Year 2019 Award," says Elena Rasmussen, Vice President Purchasing Electronics Discretes at Continental Automotive Group.



"With its focus on quality and excellent logistical support, the company is a reliable supplier to meet the challenges in a rapidly

changing market. ROHM Semiconductor is both the preferred partner for SiC technology in high voltage inverters and the company of choice in terms of power supplies. We look forward to continuing our close and trustful cooperation with ROHM in the future," adds Rasmussen.

"We are very proud to receive this award," states Toshimitsu Suzuki, President of ROHM Semiconductor Europe. "This award is a great acknowledgement of our efforts to always support our customers in achieving their business goals by providing high-quality, a stable supply of robust and advanced products as well as good services," concludes Suzuki.

www.rohm.com

**SMALLER
STRONGER
FASTER**

ROHM
SEMICONDUCTOR



REDUCES STANDBY POWER FOR ALWAYS-ON CONSUMER PRODUCTS

ROHM's BM1ZxxxFJ integrated zero cross detection IC series is optimized for home appliances such as vacuum cleaners, washing machines, and air conditioners. The device provides designers a turn-key zero cross detector without the need for a complex design using discrete components. Additionally, this integrated solution does not use a photo-coupler typically used in other solutions, and therefore, it further reduces standby current consumption and increases long-term reliability.

KEY FEATURES

- Breakthrough photocoupler-less zero cross detection circuit design minimizes application standby power consumption
- Contributes to improved reliability and efficiency in home appliances in a variety of countries and regions
- Easily replace conventional zero cross detection circuits
- Integrated voltage clamp function protects the downstream MCU



CONSUMER

www.rohm.com

AC Drives for Smart Technology Hub

Finland-based Danfoss Drives and other Danfoss business segments will supply the technology company Wärtsilä's research, product development and production center Smart Technology Hub with a significant number of AC drives and other products. Wärtsilä's Smart



Technology Hub will be completed in Vaskiluoto, Vaasa next year.

In all, 192 pieces of Danfoss AC drives with a total power of 32 megawatts will be delivered from the Danfoss Vaasa factory to Wärtsilä's testing area for products and solutions. In addition, the delivery includes VACON AC drives for various building automation applications, as well as other building automation products from Danfoss' other business segments. As Wärtsilä's technology partner, Danfoss is co-designing and delivering systems for the new testing area.

"This is a unique opportunity for Danfoss and in particular for us at Danfoss Drives in Vaasa to intensify our cooperation with Wärtsilä. We will be in an increasingly close dialogue with Wärtsilä's research and product development in the future, and in this way, we will be able to help one another with different business opportunities. In addition, Danfoss' customers will also be able to visit currently one of the most modern testing labs in the Smart Technology Hub," says Markus Forma, Global Key Account Manager for Wärtsilä at Danfoss Drives.

www.danfoss.com

One of the Most Sustainable Companies Worldwide

Infineon Technologies has again been listed in the Dow Jones Sustainability™ World Index and in the Dow Jones Sustainability™ Europe Index. This was announced by the investment specialist RobecoSAM. Thus, Infineon was ranked among the top of the world's most sustainable companies for the 11th time in a row.



"We are pleased and proud of being acknowledged as one of the top sustainable companies in the world. At the same time, it is also an encouragement to continuously develop our processes and improve our sustainability," said Dr. Sven Schneider, Chief Financial Officer at Infineon. "At the beginning of the year, Infineon has committed itself to becoming CO₂-neutral by 2030, thus taking the next strategic step towards more climate protection. Forward-looking manage-

ment, acting in an environmentally-friendly manner and social commitment are indispensable prerequisites for the resilience of Infineon and our long-term success".

Infineon has been actively contributing to better resource management, energy efficiency and effective climate protection for years. With the help of Infineon's products and solutions, 35 times more CO₂-emissions can be saved over their lifetime than had been created during production. Setting a carbon-neutrality goal for its own activities is a consequent and important next step in the company's climate protection efforts. Infineon puts a clear focus on further enhancing energy efficiency and continuously reducing CO₂-emissions in its plants. The company aims to continuously reduce its footprint while growing production at the same time. Already by 2025, emissions are to be reduced by 70 percent compared with the base year 2019.

www.infineon.com

Collaborating to Develop Battery Disconnect Switch

VisIC Technologies is pleased to announce its collaboration with AB Mikroelektronik to develop a D³GaN based high voltage solid-state battery disconnect switch with Fast Short Circuit Detection (FSCD) for future e-mobility to fulfill the functional safety requirements. "We are happy to collaborate with AB Mikroelektronik, which is a major



player in high power automotive applications with a strong experience in solid-state battery disconnect switches. This is a big advantage in developing the next step for a 400V battery switch" said Mr. Ran Soffer, VisIC VP Sales & Marketing. "Our effort to constantly serve our customers is raising the bar for high voltage, high current solutions for the EV market. Our focus for the EV industry using the D³GaN technology is enabling the future electric-drive technology to be aligned with the market needs to reduce the electric drive cost and improve its efficiency with a reliable high voltage automotive-grade technology". The collaboration with AB Mikroelektronik in the field of high voltage battery disconnect switches will benefit from the D³GaN capability of fast switching in safety-critical applications. In the event of a short circuit in the high voltage boardnet, it is mandatory to detect and disconnect the battery as fast as possible. This requires a very fast power switch and manage the short current until the short circuit is detected and disconnected.

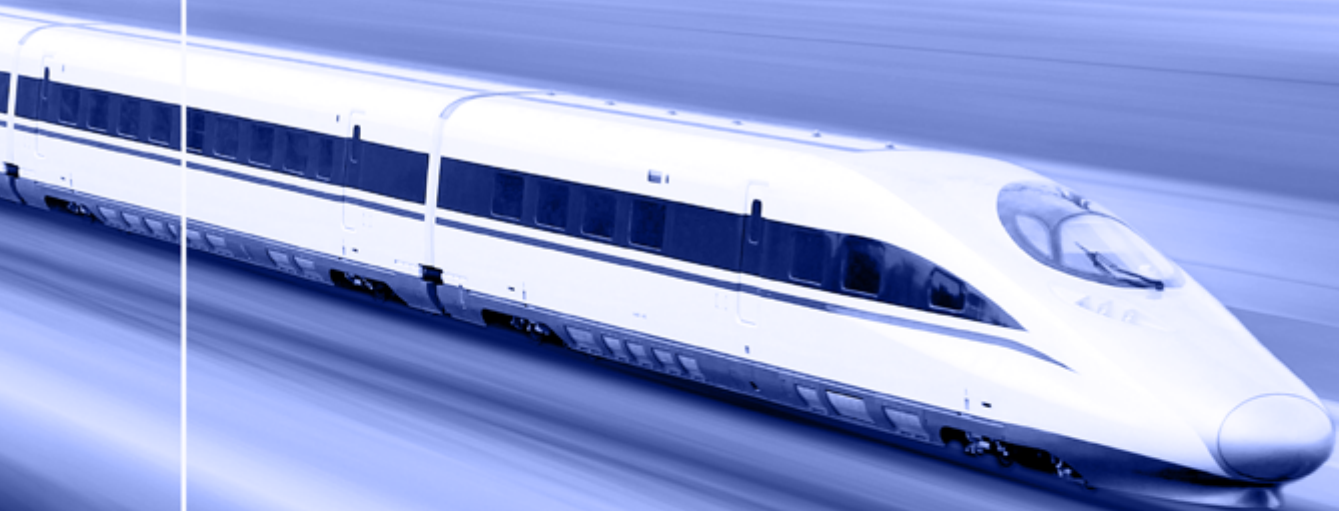
www.visic-tech.com

Shape the Future

Full SiC 3.3kV Power Module in nHPD²

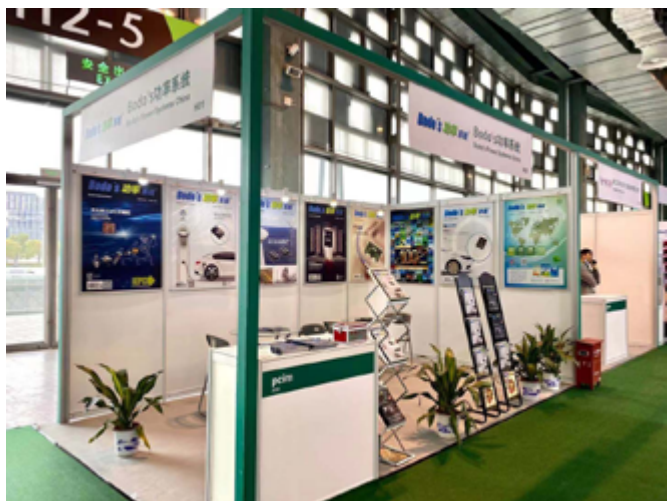
High Voltage
IGBT

**nH
PD²**



PCIM Asia 2020 Concluded Successfully

PCIM Asia was successfully held from 16 – 18 November at the Shanghai World Expo Exhibition and Convention Center. The show welcomed a total of 69 exhibitors who presented the latest trends, developments and product innovations for all applications of power electronics on an exhibition area of 7,000 square meters. This year's



fair saw the participation of well-known domestic and international companies such as Mitsubishi Electric, Semikron, Fuji Electric, Infineon, Beijing Sinking, Bronze, CRRC, Hangzhou Firststack, Heraeus, Keysight, Shanghai Eagtop, Toshiba and Wuxi CRE New Energy. What's more, the Korean Pavilion debuted at the fair and featured a number of South Korea's premier semiconductor companies, including Busan Techno Park Foundation, JMJ, PowerCubeSemi, SemiPowerEx and SIGETRONICS. Each of these companies' presence at PCIM Asia underlined the fair's position as one of the most significant trade platforms for power electronics in China. Fair's exceptional quality draws acclaim from participants Exhibitors were highly satisfied with the excellent quality of attendees and the plentiful networking opportunities that were offered, noting that the fair was an ideal platform to grow their businesses. Many of them also used their visit to PCIM Asia to learn more about the current market conditions and forward-looking trends and technologies in power electronics through the exhibition and conference. On the other hand, the fair attracted 4,348 trade visitors, with many praising the fair for offering them opportunities to source from a wide range of quality suppliers and gather the latest market intelligence.

www.pcimasia-expo.com

eBook Showcases High-Performance Power Conversion Components

Mouser Electronics announces an eBook in collaboration with Bourns, exploring best practices for working with power conversion components. In "Achieving Enhanced Performance and Reliability", Bourns and Mouser offer a series of technical articles designed to help readers choose the right components for specific power applications, including multiple related to high-voltage energy storage.

The growing importance and prevalence of technologies such as electric vehicles, renewable energy sources, and advanced communications networks require reliable components to support developments in energy storage and power conversion. "Achieving Enhanced Performance and Reliability", the eBook from Mouser and Bourns, presents deep dives into topics including rechargeable batteries, battery management systems (BMS) in high-voltage energy storage, and reducing winding loss in a ferrite inductor. The eBook includes convenient links and ordering information for Bourns power conversion products designed to meet the needs of these emerging technologies. The SRP-C high-current, shielded power inductors meet



the high density current requirements of modern consumer electronics applications, offering low buzz noise for DC/DC converters and power supplies. Bourns' SRP0xxx shielded power inductors feature a metal alloy powder core and flat wire, delivering exceptional temperature stability, low core loss, and low DC resistance.

www.mouser.com

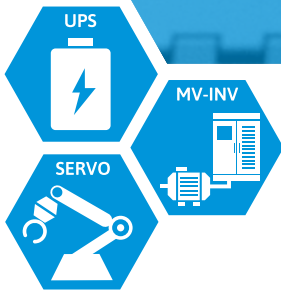
Strategic Partnership with Valuetronics

Indium Corporation and Valuetronics International have formed a strategic partnership to serve customers in the Americas with its cored wire, rework fluxes, and bar solder products. The partnership with Valuetronics, a well-known distributor of test and laboratory equipment markets, will help bring Indium Corporation's proven materials to hand assembly and rework customers. "We are eager to work with Valuetronics to continue to deliver our high-quality products and technical expertise to our customers in the Americas," said Greg Hayes, Southeast Regional Manager



and Americas Distributor Manager. Valuetronics was founded in 1992 as a seller and buyer of used test equipment and later grew to include several distribution lines of new equipment. A supplier of electronic test equipment to large, medium, and small businesses, Valuetronics stocks thousands of instruments at their Elgin, Ill. facility with a growing customer base of more than 100,000 global contacts.

www.indium.com



Industrialized process for pre-pasted Thermal Interface Material (TIM)

FEATURES

- ▶ Optimized for Fuji modules
- ▶ Increased lifetime of IGBT
- ▶ Advanced IGBT power density
- ▶ Thermal – Benefits
 - Higher thermal conductivity
 - Uniform thermal resistance
 - Increased reliability and lifetime
- ▶ Process – Benefits
 - Outsourcing of a “dirty” process
 - Stable quality level
 - Computer controlled automated process
 - Increased System reliability
 - Printing according customer specification
 - TIM upon customers preference possible

Expanded Supercapacitor Initiative

Cornell Dubilier Electronics announces the expansion of its supercapacitor operations and personnel to meet the explosive growth in applications for this rapidly evolving technology. The company's supercapacitor strategy will be under the direction of their recently hired Business Unit Manager, Brendan Andrews, who previously led sales and marketing efforts for several of the major well-known brands in supercapacitors. The company plans to introduce new products in the coming year, including cutting-edge LiC hybrid types, which offer higher operating voltages and greater energy densities. With their massive storage capabilities, supercapacitors bridge the gap between conventional capacitors and batteries providing instantaneous bursts of power that are problematic for conventional capacitors or batteries. These components are typically used individually or in series-parallel banks for power hold-up during brief interruptions to line power. In some applications, they supplement batteries or are used in place of batteries for applications as diverse as solar and wind energy harvesting, mechanical actuators, AGV (Automated Guided Vehicles), EV transportation power, smart utility meters, IIoT, pulse battery pack alternatives, memory backup, battery/capacitor hybrids, UPS systems, emergency lighting, LED power and solar lighting. CDE is moving beyond stocked components by expanding capabilities in standard



and custom packages to meet higher voltage and current application requirements. Some solutions use series-parallel banks of capacitor cells with active or passive balancing circuits. Included CDE's expansion plans are additional personnel and equipment for the advanced testing of these devices.

www.cde.com

Organisational and Personnel Changes

Isabellenhütte is restructuring its management team. In future, three managing directors will be responsible for the respective areas as CFO, CTO and CEO. Dr Felix Heusler, managing partner in the eighth generation of Isabellenhütte, explains the reason behind this change: "We see our family business confronted with rapidly changing markets in an increasingly globalised world. We intend to continue on our path of sustainable growth that we have been following for several years by expanding our product portfolio and through an even more consistent and individualised focus on customers. We are taking this development into account in our management by dividing the management team even more clearly into three units and placing the responsibilities into the hands of each managing director." Moving forward, Isabellenhütte will be managed by a three-person team, consisting of a CFO, a CTO and a CEO. As CFO, Dr Felix Heusler will be responsible for human resources (HR), finance/controlling and IT. Holger Spiegel, 53, joined the management team in July 2020 and took over responsibility for sales and marketing from Dr Felix Heusler on 1 October 2020. In addition, Holger Spiegel will act as speaker for the management team (CEO) from 1 January 2021.



Since 1 November 2020, Thilo Gleisberg, 51, has been the third and final member of the management team. In his role as CTO, he is responsible for production, R&D, procurement and logistics. The company would like to thank managing director Jürgen Brust, who will retire on 31 December 2020. During his time at the company, Isabellenhütte has developed into a globally recognised technology leader.

www.isabellenhuetten.de

2020 Global Semiconductor Alliance (GSA) Award



Vicor won the 2020 Global Semiconductor Alliance (GSA) Award for Analyst Favorite Semiconductor Company. Vicor high-efficiency, high-density power system solutions enable advances in artificial intelligence and other demanding applications. Vicor was among five companies nominated in this category including AMD, NVIDIA, Inphi Corporation and SiTime Corpora-

tion. Semiconductor financial analysts from two top-tier firms selected their favorite semiconductor company for this award. The analysts based their decision on historical as well as projected data such as stock price, earnings per share, revenue forecasts and product performance. The 2020 GSA Awards recognize leading semiconductor companies that have exhibited market growth through technological innovation and exceptional business management strategies.

www.vicorpower.com



RT BOX 1:
THE ORIGINAL

RT BOX 2:
MULTI-CORE

RT BOX 3:
HIGH I/O COUNT

THE REAL-TIME FAMILY HAS GROWN

Building blocks for HIL simulation
and rapid control prototyping

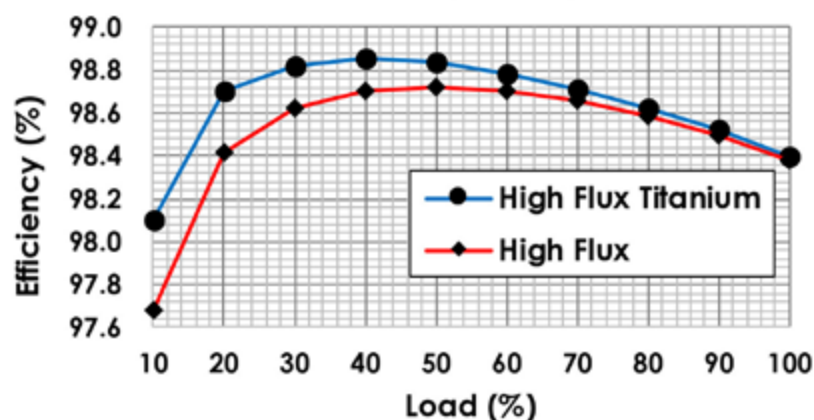
High Flux Titanium Series (GT Grade)

Chang Sung Corporation has successfully launched upgraded High Flux Core called HIGH FLUX TITANIUM Series (GT Grade), which is a High Flux material born by innovative manufacturing process. Of all the power applications, HIGH FLUX material is specialized in server and telecom power supply units and on-board charger for EV cars where require high efficiency. HIGH FLUX GT equipped with excellent flux density and core loss property is the best material for PFC and output inductors. Recently, the introduction of SiC and GaN leads to an increase in switching frequency and results in the miniaturization of

power modules. Under the high switching frequency, low core loss, in particular, low eddy current loss, is very much important for inductors to get high efficiency and low temperature in devices. High Flux GT, CSC's grant achievement, which has about 25% lower core loss at 200kHz compared to the original HIGH FLUX material will allow users to optimize their inductor designs.

www.csc-mrc.com

3kW PFC Efficiency Comparison



Material	Efficiency @50% Load
HIGH FLUX GT 60μ	98.83%
HIGH FLUX 60μ	98.72%



Core Loss

$$P_{total} = P_h + P_e$$

(P_h : hysteresis loss / P_e : eddy current Loss)

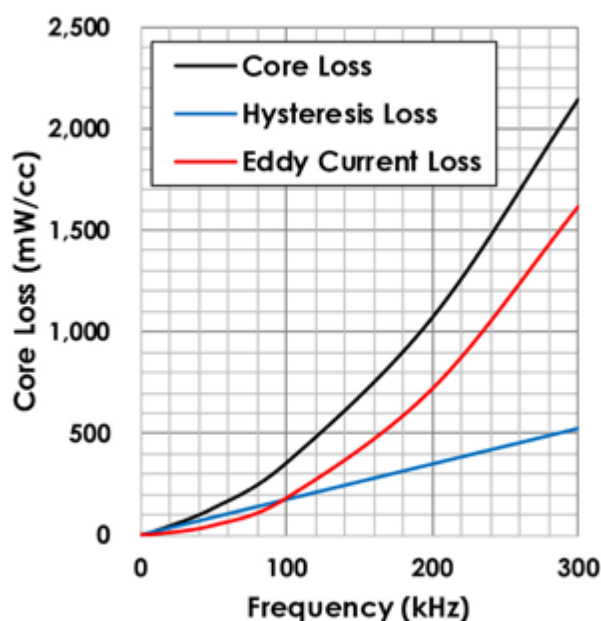
$$*P_h = K_h f B$$

(K : Constant / f : frequency / B : peak magnetic field)

$$**P_e = K_e d^2 B^2 f^2$$

(d : thickness of the material)

Core Loss Analysis





Vincotech

THE TANDEM SOLUTION FOR FASTER SWITCHING

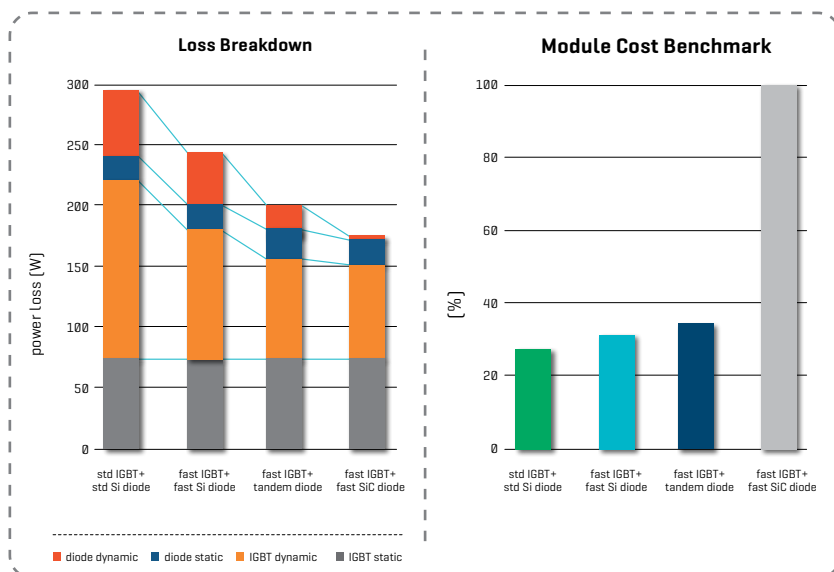


OUT NOW: 1200 V *flowPACK 1*
25 A to 75 A @ 25°C

Servo applications and line converters for elevator drives demand switching frequencies up to 16 kHz. Vincotech's new 1200 V Sixpack family based on **tandem diode concept** will ensure your designs easily meet these requirements while improving efficiency and slashing systems costs.

Main benefits

- / High-speed IGBT4 drives down switching losses
- / 650 V diodes in **tandem configuration** cut the switching losses even further
- / Integrated thermal sensor makes it so much easier and cheaper to measure temperature
- / Kelvin emitter enhances current control and switching performance
- / Standardized footprint for easier and cheaper PCB design



IGBT Module Contributes to Energy Saving in Railway Transportation

Fuji Electric has started mass production of its HPnC module outfitted with a 7th generation X-Series IGBT, targeting the railway market. The HPnC is equipped with the latest 7th-generation IGBT that boasts some of the best low-loss performance in the industry. By optimizing the structure of the package, Fuji Electric reduced the internal inductance, which interferes with high-speed switching, by 76% compared to the conventional products, resulting in low losses. An inverter equipped with the new HPnC reduces power losses during operation by about 8.6% compared to the conventional product (Fuji Electric's High Power Module). Also, combined with the improved heat dissipation described in the next chapter, it reduces heat generation, resulting in a 19% reduction in size and a 13% reduction in weight compared to the conventional product.



★Dotted lines (- -) indicate equipment on which this product is installed.

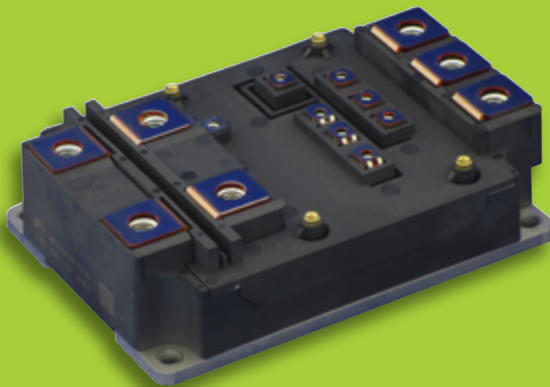
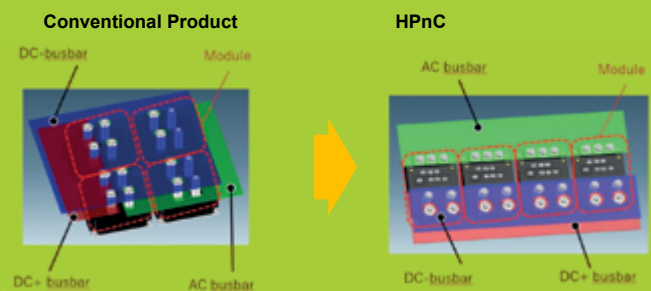


Figure 1: The HPnC IGBT Module

Package type	HPnC
Model No.	2MBI1000XVF170-50
Rated voltage	1700V
Rated current	1000A
Circuit configuration	2in1
Dimensions WxD (mm)	100x144

One of the main causes of IGBT module failure is the deterioration of the interfaces between the different components due to the stress caused by temperature changes during operation. Given this, Fuji Electric has changed the base plate material from the conventional composite of aluminum and silicon carbide (AlSiC) to a composite of magnesium and silicon carbide (MgSiC), thereby improving the heat dissipation and lowering the stress caused by thermal changes. In addition, the terminals of the new module are attached to the insulation substrate by ultrasonic bonding as opposed to the solder joint in the conventional module, thus reducing the failure rate.



The conventional product requires three separate bus bars (conductors for electrical connection; DC+, DC- and AC bus bars) that overlap each other when constructing a circuit, making the wiring configuration complicated when using parallel connection of power semiconductors. Optimizing the terminal arrangement of this product has made it possible to arrange three types of bus bars in the same direction, easily facilitating parallel (multiple) connection of power semiconductors and contributing to improved assembly for various inverters.

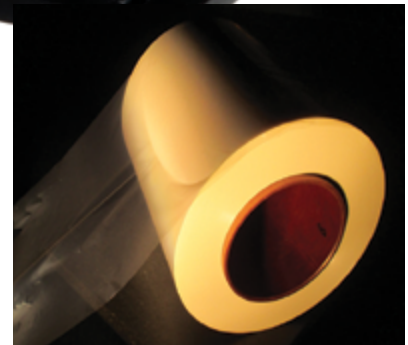
www.fujielectric-europe.com

www.americas.fujielectric.com/semiconductors



906A107
Integrated Capacitor
Assembly
with Bus

ENABLING A 75% RATING INCREASE WITH NO CHANGES TO THE COOLING*



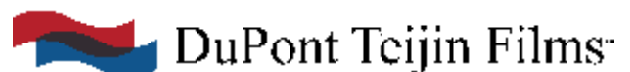
DuPont Teijin Films
Kaladex® PEN HV™

Where conventional polypropylene can only operate up to 107 °C, Kaladex® PEN HV™ film, manufactured by DUPONT TEIJIN FILMS and wound by ADVANCED CONVERSION, for integration into the DC link, allows operation up to 130 °C which enables a 75% rating increase with no changes to the cooling.

Alternatively, the cooling infrastructure can be reduced to achieve the same current rating thus reducing size, weight, and cost while increasing power density.

Contact ADVANCED CONVERSION today for your design needs.

Enabling High Temperature Operation of Optimized DC Link Capacitor/Bus Test Kit,
Bodo's Power Systems, January 2021, Page 32



1 (802) 661-3450 #100
info@advanced-conversion.com

+352 (0) 2616 4004
europe.films@gbr.dupont.com

750V Gen 4 SiC FETs Enable Higher Efficiency Power Designs

Silicon carbide adoption has accelerated dramatically in recent years, thanks to solid technological progress in the quality and performance of components, their availability, and the emergence of applications that benefit from that performance. UnitedSiC has pursued a strategy of continuous technological innovation, to deliver the lowest $R_{ds(on)}$ power components in the 650V-1200V range [1], built on the excellent characteristics and high yields of our proprietary SiC JFET technology.

By Anup Bhalla, V.P. Engineering, United Silicon Carbide Inc.

With the recent launch of the Gen 4 (G4) UJ4C SiC FET series, we open the next chapter in the expansion of SiC usage in power conversion and inverter applications with a large improvement in device characteristics, aimed at providing users with the next level of performance and system cost benefits.

Comparative characteristics of available technologies

The first UJ4C products from UnitedSiC (see Table 1) target a 750V $V_{DS(MAX)}$ rating instead of 650V, in order to tackle applications using a 500V DC Bus, while serving the traditional 300/400V bus applications. The devices maintain the $\pm 20V$ gate rating, built in ESD protection, and the ability to use simple unipolar gate drives enabled by the 5V V_{TH} , that are all features of the SiC FET's cascode architecture. In high frequency applications, gate drives as low as 0 to 10V may be used, with minimal impact on conduction loss. The ultra-low specific on-resistance of this technology (SiC JFET 0.7mohm-cm²) allows about half the resistance in a given package size relative to 650V SiC MOSFETs.

At a given resistance, the chips are shrunk, which leads to much lower capacitances. This in turn leads to lower switching losses. The TO247-3L and 4L packages use Ag sinter technology to enhance thermal resistance in conjunction with chip thinning, to mitigate the effects of the smaller JFET die, and allow excellent junction-to-case thermal resistance R_{THJC} to be achieved. The devices preserve the ability to handle avalanche events and are especially good at handling lower energy high current avalanche events up to 2X rated current. Excellent third quadrant behavior with low V_{FSD} (<1.5V) and low temperature independent Q_{RR} is another feature of SiC FETs, and G4 devices have much reduced Q_{RR} than their earlier G3 counterparts, driven by the C_{OSS} reduction.

In Table 2, we compare technological parameters for state of the art SiC MOSFETs, Superjunction devices and G4 SiC FETs. The rows showing R_{DSA} indicates the resistance mohm-cm² of active chip area at 25C and 125C. This is resistance of the JFET used to

construct the cascode SiC FET, and the additional resistance of the LVMOS may add 10% to this number. The 5V V_{TH} of the G4 SiC FET in conjunction with the 0 to 12V gate drive is unique and delivers the best available $Q_g \cdot V$ figure-of-merit for gate drive loss. Operating these devices at 500kHz-1MHz can be accomplished without overheating standard gate drivers.

The cascode construction allows for the lowest available V_{FSD} body diode drop of all the wide-band-gap options, allowing the use of these devices in non-synchronous rectification mode. Since the reverse recovery performance Q_{RR} is also excellent, the overall figure-of-merit $V_F \cdot Q_{RR}$ is unmatched for G4 SiC FETs. This allows for excellent hard switching performance and prevents device failures in ZVS circuits if hard switching occurs under any load conditions. The figures of merit $R_{DS} \cdot E_{OSS}$ and $R_{DS} \cdot C_{OSS,TR}$ based on the net cascode resistance are used to assess the fundamental capability of the technology for hard and soft-switching applications and can be seen to be best-in-class. These devices can allow a simpler implementation of higher frequency soft-switched circuits such as LLC, CLLC, DAB and PSFB.

PRODUCT	Irrated Tc100	Voltage rating	$R_{DS(on)}$ @25C	$R_{DS(on)}$ @125C	Tj (max)	Rth,j-c (max)	Qg	V_{FSD} @25C	Eoss (400V)	Coss, tr (400V)
UJ4C075018K3S UJ4C075018K4S	60A	750V	18mΩ	31mΩ	175C	0.3C/W	38nC	1.2V	12uJ	280pF
UJ4C075060K3S UJ4C075060K4S	21A	750V	58mΩ	106mΩ	175C	0.75C/W	38nC	1.3V	4uJ	54pF

Table 1: Key parameters of the first Gen 4 SiC FET products

TECHNOLOGY	G4 SiC FET	SiC MOS1	SiC MOS2	SiC MOS3	Si (fast)
Voltage Rating [V]	750	650	650	650	600
R_{dsA} @25C (mohm-cm ²) SiC	0.7	2.1	2.1	2.8	8
R_{dsA} @125C (mohm-cm ²) SiC	1.26	2.6	2.6	4.3	14.4
V_{TH}	4.8	4.5	2.3	3.1	3
Preferred Gate drive	0 to 12V	0 to 18V	-4 to 15V	-5 to 18V	0 to 10V
$Q_g \cdot V$ (uJ)	0.36	1.13	3.57	3.73	2.51
$V_{FSD}(25C)$ [V] Nominal Current, $V_{gs}Off$	1.6V(50A)	4V(38.3A)	5.4V(55.8A)	4.3V(50A)	1V
125C $R_{ds(on)} \times E_{oss}$ [mOhm-uJ]	372	732.6	714	754	826.5
125C $R_{ds(on)} \times C_{oss, tr}$ [mOhm - nF]	8.7	12.1	8.8	13.7	108.2
$V_F \times Q_{rr}$ [V-uC]	0.17	0.96	2.33	1.59	1.56
$R_{ds(on)}$, Nominal	18m	27m	15m	20m	15m

Table 2: Comparison of parameters for G4 750V SiC FETs with similar 650V SiC MOSFETs and 600V Superjunction fast diode FETs

Say Hello to the Future!

Introducing the industry's first 750V high performance SiC FETs.

- More design headroom; excellent for 400/500V bus
- RDS(on): 18mΩ/60mΩ
- Superior performance and efficiency
Figures of Merit
 - Best-in-class RDS(on) x Area delivers 45-75% lower conduction losses for a given footprint and package type
 - Hard switched: Lowest total losses based on low Eoss / Qoss x RDS(on)
 - Soft switched: Low RDS(on) x Coss(tr) enables higher power density
- Driven with gate voltages compatible with SiC MOSFETs, Si MOSFETs or IGBTs
- TO-247 in 3-lead & 4-lead Kelvin source
- AEC-Q101 qualified



Learn more at unitedsic.com/gen4



Watch and Share Video

Learn how to increase power design efficiency with new Gen 4 SiC FETs.



Read Technical Product Overview

See how our Figures of Merit achieve unmatched performance.

Switching waveforms and managing switching speed

Figure 1 shows the half-bridge switching waveforms of the 60mohm and 18mohm 750V devices in a TO247-4L package measured at 400V, 20A and 50A respectively. Waveforms are shown with comparing a large R_g to control the turn-on and turn-off vs. using a RC snubber across the device with a low R_g at the gate. Both circuits employ a RC snubber from the DC bus to ground, referred to as a bus snubber [2].

The upper row of Figure 1 shows the switching behavior of the 60m, 750V SiC FET UJ4C075018K4S. The difference in turn-on loss using just an $R_g=25\Omega$ (171uJ) vs a low R_g of 1ohm along with a 10hm, 95pF drain-source RC snubber (142uJ) is small. The turn-on di/dt is significantly slower with the $R_g=25\Omega$, but the peak recovery current is not much different. The maximum dV/dt during turn-on is similar, since it is set by the SiC JFET, and not altered by the R_g applied to the LV MOSFET in the SiC FET. The turn-on delay is higher with the 25ohm R_g .

The turn-off behavior for the cases using a 20ohm R_{goff} (37uJ), vs. a R_{goff} of 1ohm along with a 10hm, 95pF drain-source RC snubber (17uJ), shows that using a snubber, lower losses can be obtained, while preserving a short turn-off delay and somewhat lower VDS overshoot and reduced ringing. The losses shown include the snubber

loss, which is separately extracted in the datasheet, and is very small [2, 3]. However, at lower currents like 20A, the snubber is not needed in many applications, since the added losses with simple R_g control are not excessive. The use of bus snubbers is still recommended, since it improves ringing performance with minimal loss impact.

At 50A however, the waveforms using snubbers are far superior and allows a reduction in $E_{ON}+E_{OFF}$ total switching loss by nearly 36%. Using the low R_g , delay times can also be kept low. In the lower curves in Figure 1, the switching data at 50A, 400V for the UJ4C075018K4S (18m, 750V) is compared for the cases using a 25ohm R_{goff} /50ohm R_{goff} vs. a $R_g=1\Omega$ with a 10ohm, 300pF RC snubber across the drain-source of each device. The low R_g of 1ohm can only be used if the snubber is in place to manage the overshoots and ringing. This arrangement allows switching at a much faster di/dt with reduced turn-on delay time. The turn-on loss (including snubber loss) is now seen to be 418uJ vs 483uJ driven by the faster operating di/dt. Note however, that this faster di/dt did not come with any significant increase on peak recovery current.

Similarly, the 50A, 400V turn-off waveforms in the bottom right of Figure 1 show that the much faster switching and reduced delay time with the $R_g=1\Omega$ plus RC snubber case is achieved without excessive VDS overshoot or phase node ringing. The turn-off delay

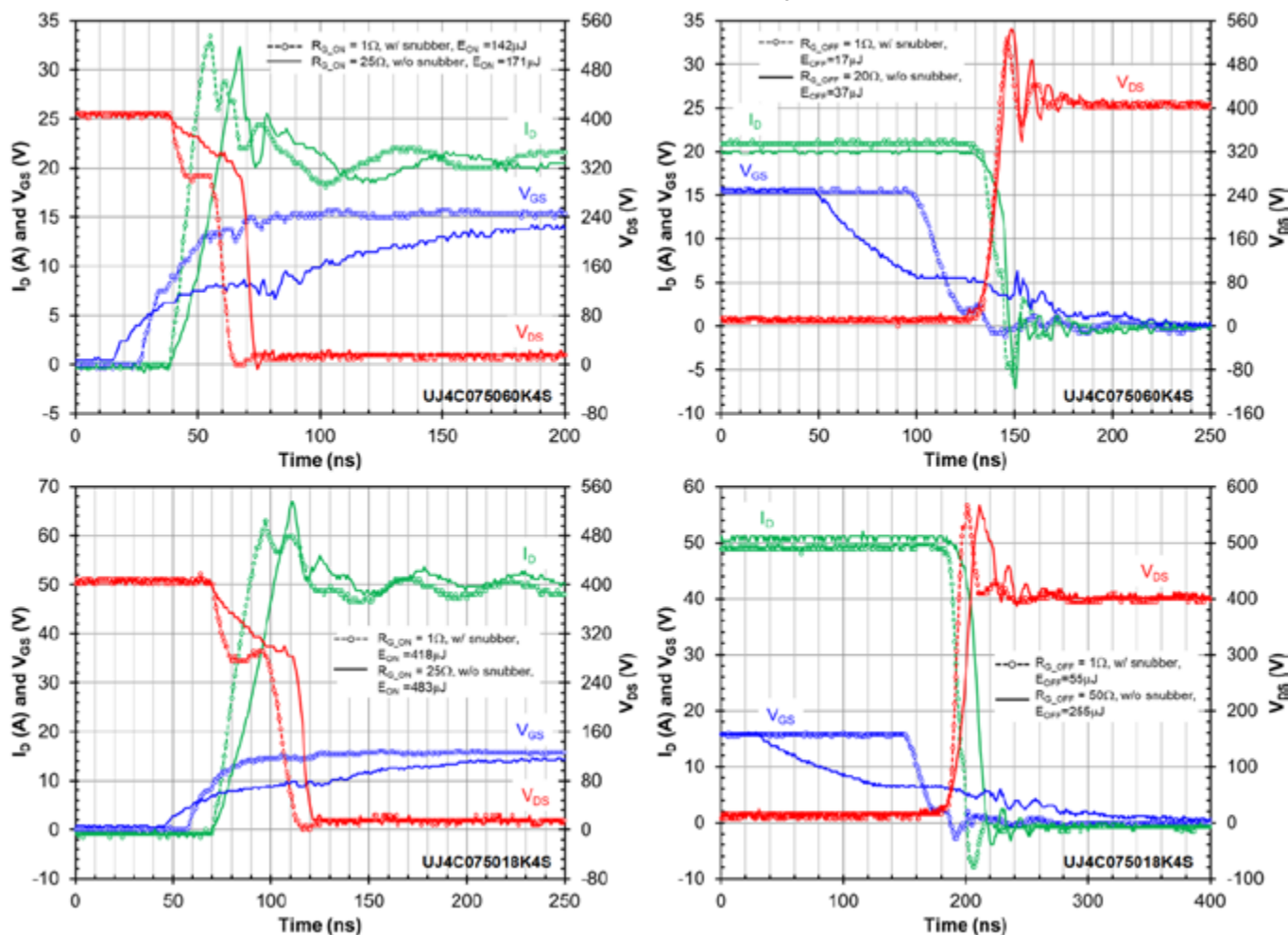


Figure 1: Half bridge-switching waveforms for the G4 SiC FET products. The upper row shows the behavior of the 60m, 750V device at 20A, 400V while the lower row shows the behavior of the 18m, 750V device at 50A, 400V. The left column shows the turn-on waveforms, the right column shows the turn-off waveforms. The dashed lines use a low external R_g along with a RC snubber on the PCB between drain-source for each device, while the solid lines use high external R_g values to slow down switching. In all cases, a bus snubber is utilized, i.e. a resistance in series with the bus de-coupling ceramic capacitors (2.5ohm, 100nF) and a 0 to 15V gate drive is used.

time is kept very short as well. Given that the E_{OFF} with the $R_g=1\Omega$ hm with RC snubber is just 55 μ J compared to the 255 μ J when a 50 Ω hm resistor is used to bring down the voltage overshoot to a comparable level, it is clear that using the snubber is very advantageous for higher current applications >20A.

The exact choice of snubber can be dependent on the application, overall circuit inductances, and peak current levels for turn-off, and may not be necessary if the currents are below 25A. The loss in the snubber resistor is best measured directly by integrating the V^2/R loss at turn-on and turn-off. These values are indicated in the product data-sheets [2] and are 1.7 μ J at 20A, 400V for the UJ4C075060K4S with a 10 Ω hm, 95pF snubber and 9.5 μ J at 50A, 400V for UJ4C075018K4S with a 10 Ω hm, 300pF snubber.

It is recommended that the device simply use a 0 to 12V or 15V gate drive, although with appropriate changes to R_g values [4], -5V to 15/18/20V and other common gate voltage rails may all be used. Often 0 to 10V is employed when switching above 300kHz.

Figure 2 compares the half-bridge switching waveforms for the 18m, 750V device and 60m, 750V device using the TO247-4L vs TO247-3L package, with 0-15V gate drive, using only a bus snubber. The upper

row shows the turn-on and turn-off waveforms for the 60m, 750V device using a the same $R_{gon}=1\Omega$ hm, $R_{goff}=20\Omega$ hm for both devices. The solid lines are for the 3L package, while the dashed lines are for the TO247-4L.

The faster turn-on di/dt is, of course, expected for the TO247-4L since the common-source inductance is bypassed, leading to lower E_{ON} despite a higher current peak. The gate V_{GS} ringing is much improved using the TO247-4L. V_{GS} ringing for the TO247-4L is also better at turn-off, although here, the peak V_{DS} overshoot is lower with the 3L package along with a higher E_{OFF} .

The lower half of Figure 2 looks at the use of the two package types for 50A, 400V switching of the 18m, 750V device in a half-bridge, each with a 10 Ω hm, 300pF snubber, $R_g=1\Omega$ hm and 0-15V gate drive. There is now a much larger difference in the waveforms and switching losses between the 3L and 4L package types. The 3L devices have significantly higher turn-on (1.67x) and turn-off loss (4X) with similar V_{DS} overshoot and dV/dt s, and with greater V_{GS} ringing, especially at turn-off. Clearly, for using TO247 packages at higher currents, using the combination of the 4L package with the device RC snubber allows for peak performance with well managed switching waveforms.

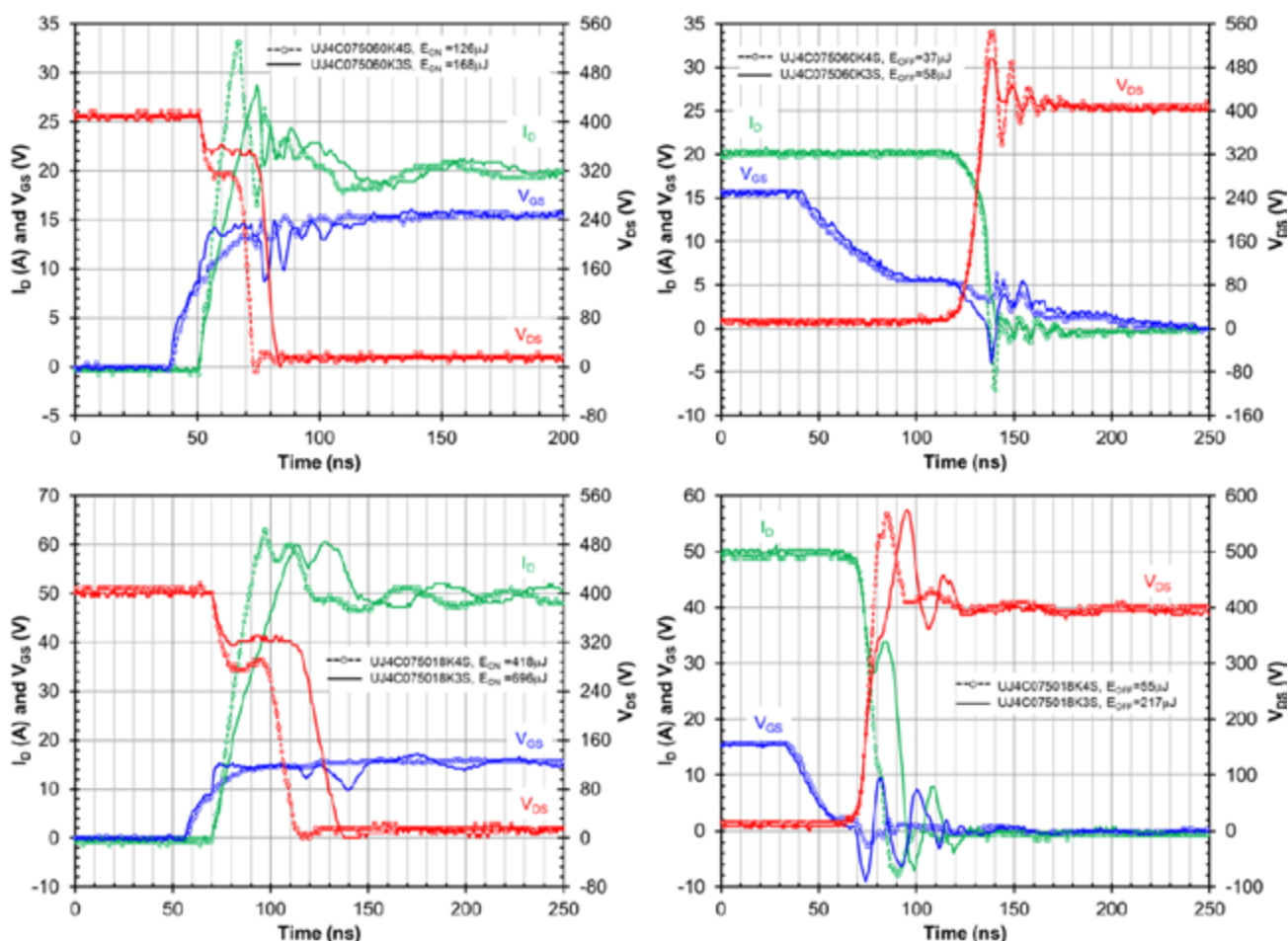


Figure 2: Half bridge-switching waveforms for the G4 SiC FET products in TO247-3L vs TO247-4L packages. The upper row shows the behavior of the 60m, 750V device at 20A, 400V while the lower row shows the behavior of the 18m, 750V device at 50A, 400V. The left column shows the turn-on waveforms, the right column shows the turn-off waveforms. The dashed lines are used for the Kelvin source K4S TO247-4L package, while the solid lines are used for the K3S standard TO247-3L package. In all cases, a bus snubber is utilized, i.e. a resistance in series with the bus de-coupling ceramic capacitors (2.5 Ω hm, 100nF) and a 0 to 15V gate drive is used. For the upper row, the 60m, 750V devices in the two packages are measured with $R_{gon}=1\Omega$ hm, $R_{goff}=20\Omega$ hm, but without any RC device snubber. In the lower row, given the high 50A, 400V switching, a 10 Ω hm, 300pF drain-source snubber is applied across each 18m, 750V SiC FET and an $R_g=1\Omega$ hm is used.

Overview of Application Benefits

We can now look at how these features of G4 SiC FETs impact a range of device applications. Figure 3a shows an example of using the 60m, 750V in a 3.6KW Totem Pole PFC circuit. The semiconductor efficiency plotted is calculated from the measured conduction and switching losses of the devices, accounting for the temperature rise, but not including controller, inductor or other system losses. The low conduction and switching losses, excellent diode recovery, and simple gate drive leads to the high efficiency seen here. This efficiency meets or beats that achievable by costlier SiC MOSFET options that require more complex gate drives. Both the 3L and 4L versions of the TO247 package are supported. Figure 3b shows the same data, comparing the efficiency with the slow leg of the TPPFC replaced with a Si rectifier diode instead of a SiC FET. The Si diode option is more

cost effective, saving two transistors and gate drives, but a 0.2% drop in efficiency occurs at high line. While one 60mohm FET is sufficient for 1.5KW applications, one unit of the 18mohm, or two of the 60m paralleled are best for 3 to 3.6KW. The single 18mohm device option requires lower gate drive power and consumes less space.

Table 3 is a similar estimation of semiconductor losses using the 60m and 18m, 750V SiC FETs in a 3600W LLC application. The conduction, gate drive, and diode losses are added to estimate the net loss per device at maximum load. Using either 2 paralleled 60m SiC FETs or a single 18m SiC FET, losses can be kept under 6.3W per FET even at 500kHz, allowing for very high efficiency with minimal need for heat sinking. While losses are dominated by conduction losses, the relative contributions of turn-off, gate drive and diode conduction losses are also shown, and are seen to be very low using the characteristics of the G4 SiC FET.

The use of UnitedSiC FETs provide a simple path to higher efficiency in these soft switched applications without much need to change the gate drive. In this case, when ZVS operation is lost, the ability of the device to hard switch without poor diode recovery ensures no failures occur. The additional voltage headroom also helps with longer field life when that is needed.

Summary

In this article, we reviewed the parameters of the new G4 UJ4C 750V SiC FETs from UnitedSiC compared to SiC MOSFETs and Superjunction FETs in the 600/650V class. We then delved into the switching characteristics of devices in both the TO247-4L and TO247-3L packages and demonstrated the benefits of using the TO247-4L package and for currents >25A, the value of RC snubbers to manage switching waveforms while minimizing losses. We used the known device parameters to extract the losses both in a Totem-Pole PFC and an LLC example, showing how these devices can allow a path to 80Plus Titanium efficiency with a simple gate drive implementation. The advantages in both hard and soft-switched applications, coupled with the easier gate drive and the extra 100V margin, make this a compelling new entry in the rapidly expanding universe of SiC transistors targeting the 600-750V range of applications in EV chargers, EV DC-DC converters, Datacenters, Telecom power, Renewable energy and Energy storage. A wealth of additional information can be found on the UnitedSiC website [2,3,4].

References

- [1] <https://chargedevs.com/newswire/unitedsic-announces-sic-fets-with-rds-on-of-less-than-10-mohms/>
- [2] https://unitedsic.com/datasheets/DS_UJ4C075018K4S.pdf; https://unitedsic.com/datasheets/DS_UJ4C075060K4S.pdf
- [3] Minimizing EMI and switching loss for SiC FETs. <https://www.youtube.com/watch?v=HhV-SS-AnwI>
- [4] <https://unitedsic.com/guides/UnitedSiC%20SiC%20FET%20User%20Guide.pdf>

www.unitedsic.com

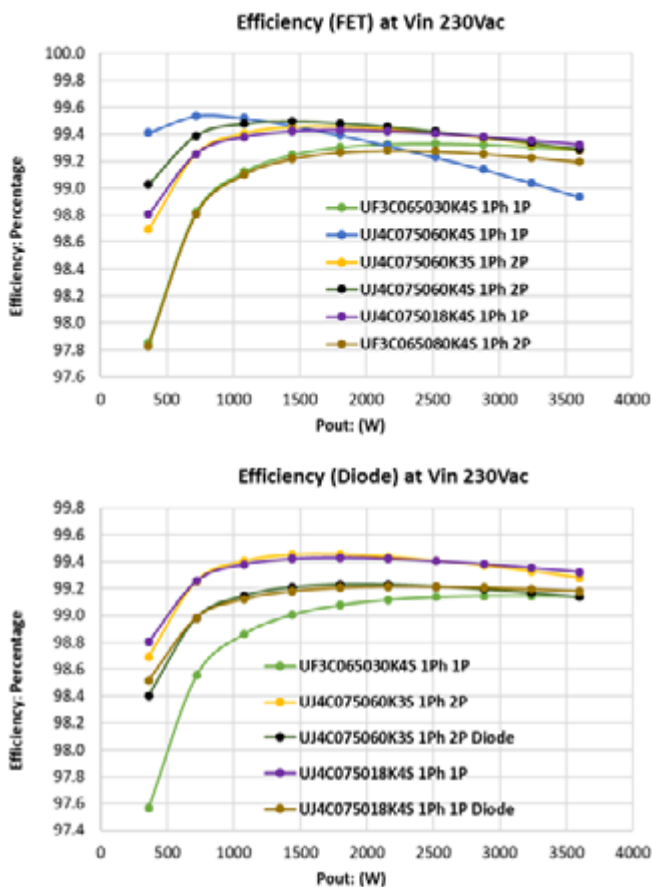


Figure 3: Semiconductor efficiency using various SiC FETs in a Totem-Pole PFC circuit at 65kHz accounting only for the losses in the power device. The plot on the left uses SiC FETs for both the fast switching and slow switching legs, while the plot on the right compares the difference using SiC FETs on the fast leg (1x UF3C065030K3S), with Si rectifier diodes on the slow leg. The Si diode option reduces efficiency by about 0.2%. The term 1Ph 2P indicates 1 Phase with 2 parts in parallel. UF3C devices are G3 devices, included here to show the performance relative to UJ4C G4 devices.

Pout (W)	Device	# of Devices in Parallel	fsw (kHz)	Pcond (W)	Poff (W)	Pgate (W)	Pdiode (W)	Loss per device (W)
3600	UJ4C075060K3S	1	300	24.08	2.35	0.11	0.88	27.42
		2	300	3.88	0.37	0.22	0.53	5.00
		2	500	3.89	0.62	0.36	0.88	5.75
3600	UJ4C075018K4S	1	300	4.37	0.58	0.11	0.45	5.51
		1	500	4.37	0.97	0.18	0.75	6.27

Table 3: Semiconductor losses in a 3600W LLC circuit using G4 SiC FETs at various frequencies. Very high efficiencies are possible, with each device contributing <6.27W losses even at 500kHz



Replaces 3 or more wet tantalum capacitors in parallel or series

Superior capacitance retention at -55°C

Less weight and requires less space

Rugged stainless steel case withstands up to 80g's

Glass-to-metal seal prevents dry-out for exceptionally long life

YOUR MISSION-CRITICAL APPLICATIONS REQUIRE SLIMPACK PERFORMANCE

MLSH Slimpack is designed to meet the most demanding military and aerospace applications. It's the world's only hermetic aluminum electrolytic capacitor with a glass-to-metal seal. Slimpack delivers extremely high capacitance at ultra-low temperatures. Energize your next idea with MLSH Slimpack.

cde.com/MLSHSlimpack

Layout Considerations for GaN Transistor Circuits

Gallium nitride (GaN) transistors have been in mass production for over 10 years. In their first few years of availability, the fast switching speed of the new devices – up to 10 times faster than the venerable Si MOSFET – was the main reason for designers to use GaN FETs.

By Alex Lidow Ph.D., CEO and Co-founder, Efficient Power Conversion

Introduction

As the pricing of GaN devices normalized with the MOSFET, coupled with the expansion of a broad range of devices with different voltage ratings and power handling capabilities, much wider acceptance was realized in mainstream applications such as DC-DC converters for computers, motor drives for robots, and e-mobility bikes and scooters. The experience gained from the early adopters has led the way for later entrants into the GaN world get into production faster.

This article is the first in a series of articles discussing three topics that can help power systems designers achieve the most out of their GaN-based designs at the lowest cost. The three topics are: (1) layout considerations; (2) thermal design for maximum power handling; and, (3) EMI reduction techniques for lowest cost.

Parasitic Inductance Due to the High Switching Speed of GaN

The use of GaN at higher frequencies than the aging power MOSFET is capable has put a spotlight on the degrading effects of parasitic inductance in a power conversion circuit [1]. This inductance hinders the extraction of the full benefit of GaN's extra-fast switching capabilities with reduced EMI generation. For a half-bridge configuration, which is used in about 80% of power converters, the two main sources of parasitic inductance are: (1) the high-frequency power loop formed by the two power switching devices along with the high-frequency bus capacitor and, (2) the gate drive loop formed by the gate driver, power device, and high-frequency gate drive capacitor. The common source inductance (CSI) is defined by the part of the loop inductance that is common to both the gate loop and power loop. It is indicated by the arrows in Figure 1.

Minimizing Parasitic Inductance

The minimization of all parasitic inductances is vital when considering the layout of high-speed power devices. It is not possible to reduce all components of inductance equally, and therefore, they must be addressed in order of importance, starting with common source inductance, then power loop inductance and, lastly, gate loop inductance.

For high-voltage PQFN (Power Quad Flat No lead) MOSFET packages, the need for a separate gate-return source pin is well known and is also implemented in high-voltage GaN PQFN structures [2,3]. When these separate pins are available, the gate drive loop and the power loop are separated within the package and extreme care must be taken in how they are connected externally.

The reduction in common source inductance comes at the expense of external source inductance, pushed outside the gate loop. This external inductance can lead to increased ground bounce due to the improved speed of the device once common source inductance is removed [4].

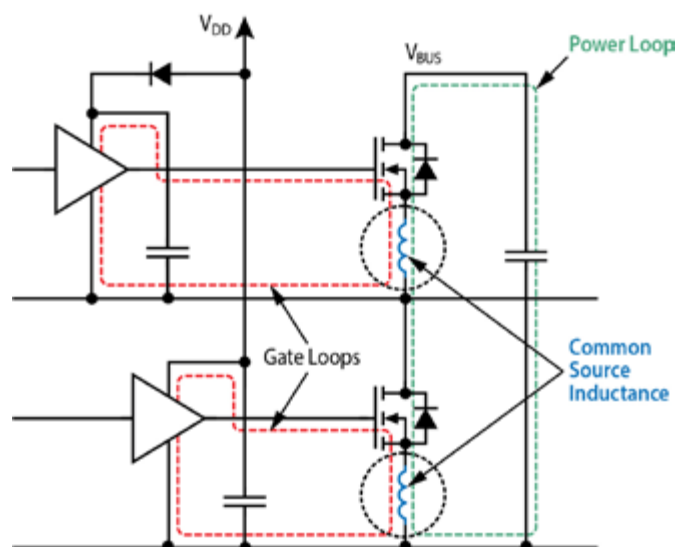


Figure 1: Schematic of a half-bridge power stage showing power and gate drive loops with common source inductance shown in dotted circles

Enhancement-mode GaN transistors are available in a Wafer Level Chip-Scale Package (WLCSP) with terminals in a Land Grid Array (LGA) or Ball Grid Array (BGA) format. Some of these devices do not offer a separate gate-return source pin, but rather a number of very low inductance connections as shown in Figure 2. The total package inductance of these packages is often less than 100 pH. This greatly reduces all components of inductance, and thereby reduces all inductance-related problems. These LGA and BGA packages can be treated in the same way as ones provided with a dedicated gate return pin or bar by allocating the source pads closest to the gate to act as the "star" connection point for both the gate loop and power loop. The layout of the gate and power loops are then separated by having the currents flow in opposite or orthogonal directions as shown in Figure 2.

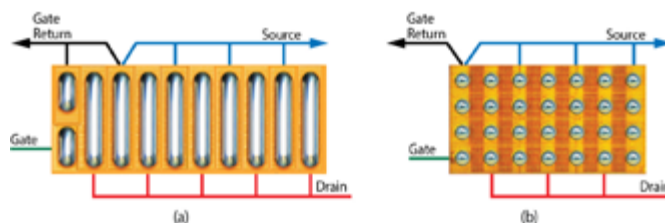


Figure 2: GaN transistors in LGA (a) and BGA (b) formats showing the direction of device current flow that minimizes common-source inductance

While minimizing the inductance of the individual elements that make up the loop (i.e. capacitor ESL, device lead inductance, and PCB interconnect inductance) is important, designers must also focus on minimizing the total loop inductance. As the inductance of the loop is determined by the magnetic energy that is stored within, it is possible to further minimize the overall loop inductance by using the coupling between adjacent conductors to induce magnetic field self-cancellation.

By interleaving the drain and source terminals on one side of the device, a number of small loops with opposing currents are generated that will decrease the overall inductance through magnetic field self-cancellation. This is not only true for the PCB traces shown in Figure 3(a), but also for the vertical solder connections and the interlayer connection vias shown in Figure 3(b). With multiple small magnetic field-cancelling loops formed, the total magnetic energy, and therefore inductance, is significantly reduced [5].

A further reduction in partial loop inductance is possible by bringing both drain and source currents out on both sides of the device from the centerline and duplicating the magnetic field cancellation effect. This works by reducing the current in each conductor, thus further reducing the energy stored, and the shorter current path yields a lower inductance.

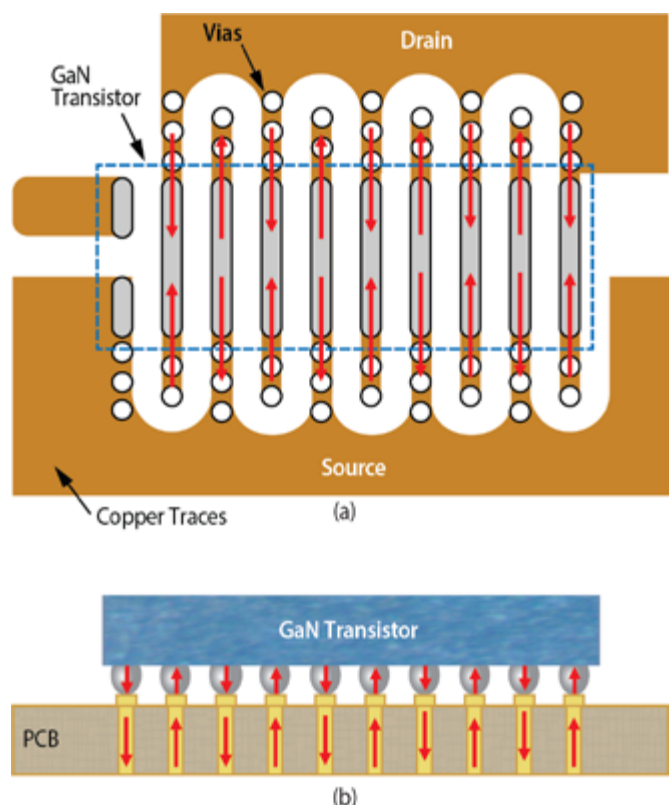


Figure 3: LGA GaN transistor mounted on a PCB showing alternating current flow (a) top view (b) side view

Conventional Power Loop Designs

To see how power loop inductance minimization can be realized in an actual layout, two conventional approaches to power loops are presented for comparison. These two approaches will be called “lateral” and “vertical” respectively.

Lateral Power Loop Design

The lateral layout places the input capacitors and devices on the same side of the PCB in close proximity to minimize the area of the high-frequency power loop. The high-frequency loop for this design is contained on the same side of the PCB and is considered a lateral power loop, since the power loop flows laterally on a single PCB layer. An example of the lateral layout using an LGA transistor design is shown in Figure 4. The high frequency loop is highlighted in this figure.

While minimizing the physical size of the loop is important to reduce parasitic inductance, the design of the inner layers is also critical. For the lateral power loop design, the first inner layer serves as a “shield layer.” This layer plays a critical role in shielding the internal circuits from the fields generated by the high-frequency power loop. The power loop generates a magnetic field that induces a current in the shield layer that flows in the opposite direction to the power loop. The current in the shield layer generates a magnetic field to counteract the original power loop’s magnetic field. The end result is a cancellation of magnetic fields that translates into a reduction in parasitic power loop inductance.

Having a complete shield plane in close proximity to the power loop yields the lowest power loop inductance for the lateral layout. This approach is strongly dependent on the distance from the power loop to the shield layer contained in the first inner layer [6]. As long as the top two layers are in close proximity, the high frequency loop inductance shows little dependence on total board thickness.

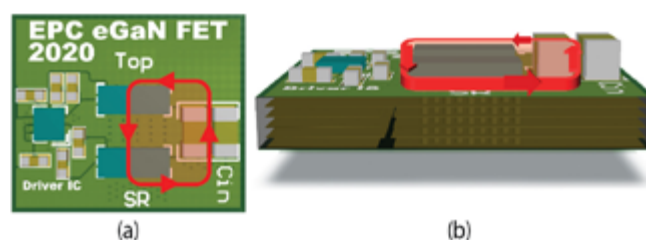


Figure 4: Conventional lateral power loop for LGA GaN transistor-based converter: (a) top view (b) side view

Vertical Power Loop Design

The second conventional layout, shown in Figure 5, places the input capacitors and transistors on opposite sides of the PCB, with the capacitors located directly beneath the devices to minimize the physical loop size. This is called a vertical power loop because the loop is connected vertically through the PCB using vias. The LGA transistor design of Figure 5 has the vertical power loop highlighted.

For this design, there is no shield layer due to its vertical structure. The vertical power loop uses a magnetic field self-cancellation method (with currents flowing in opposite directions) to reduce inductance, as opposed to the use of a shield plane.

For the PCB layout, the board thickness is generally much thinner than the horizontal length of the traces on the top and bottom sides of the board. As the board thickness decreases, the area of the loop shrinks significantly compared to the lateral power loop, and the current flowing in opposing directions on the top and bottom layers begins to provide magnetic field self-cancellation. For a vertical power loop to be most effective, the board thickness must be minimized.

Optimizing the Power Loop

An improved layout technique that provides the benefits of reduced loop size, has magnetic field self-cancellation, has inductance that is independent of board thickness, is a single-sided component PCB

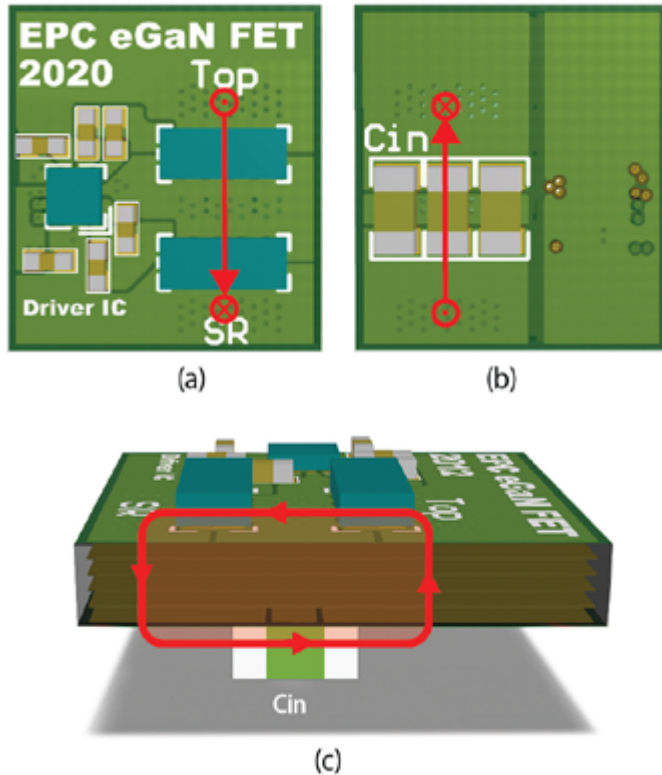


Figure 5: Conventional vertical power loop for LGA transistor-based converter: (a) top view (b) bottom view (c) side view

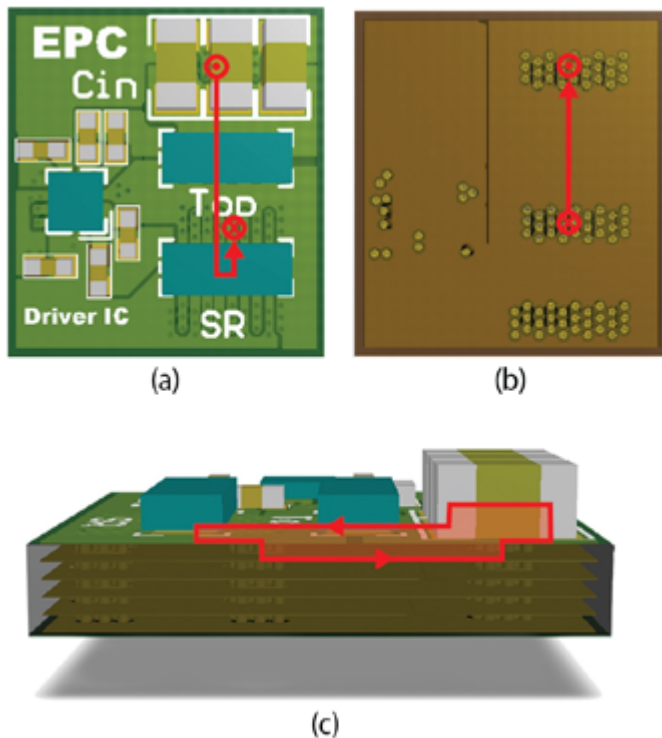


Figure 6: Optimum power loop for LGA transistor-based converter: (a) top view (b) top view of inner layer 1 (c) side view

design, and yields high efficiency for a multi-layer structure, is shown in Figure 6. The design utilizes the first inner layer, shown in Figure 6(b), as the power loop return path. This return path is located directly beneath the top layer's power loop, as shown in Figure 6(a). This positioning achieves the smallest physical loop area combined with magnetic field self-cancellation. The side view, shown in Figure 6(c), illustrates the concept of creating a low-profile magnetic field self-cancelling loop in a multilayer PCB structure.

This improved layout places the input capacitors in close proximity to the top device, with the positive input voltage terminals located next to the drain connections of the top transistor. The GaN devices are located in the arrangement as in the lateral and vertical power loop cases. The interleaved inductor node and ground vias are duplicated on the bottom side of the synchronous rectifier transistor.

These interleaved vias provide three advantages:

- The interleaving of the vias with current flowing in opposing direction reduces magnetic energy storage and helps generate magnetic field cancellation. This results in reduced eddy and proximity effects, thus reducing AC conduction losses.
- The vias located beneath the lower transistor reduces resistance and accompanying conduction losses during the transistor free-wheeling period.
- The vias reduce thermal spreading resistance, thus increasing efficiency and power handling.

The characteristics of the conventional and optimal designs are compared in Table 1.

	Lateral Loop	Vertical Loop	Optimal Loop
Single-Sided PCB Capability	Yes	No	Yes
Magnetic Field Self-Cancellation	No	Yes	Yes
Inductance Independent of Board Thickness	Yes	No	Yes
Shield Layer Required	Yes	No	No

Table 1: Characteristics of conventional and optimal power loop designs

Impact of Integration on Parasitics

To further reduce the parasitic inductance of GaN transistor-based designs, monolithic GaN power stage integrated circuits are available [7]. In Figure 7, a block diagram and actual chip photo of a monolithic power stage GaN IC is shown. The experimentally measured efficiency of this monolithic integrated circuit, shown in Figure 8, is compared against a discrete circuit using eGaN® transistors with the same on-resistance and driven by a uPI Semiconductor uP1966 Si half-bridge

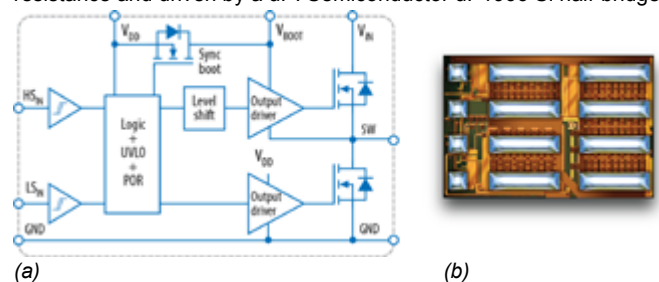


Figure 7: Block diagram for the monolithic power stage (a) and chip photo (b)

driver IC [7] in an optimal layout. The advantages of the reduced power loop and gate loop inductances in the GaN IC becomes clear as the overall efficiency gain from integration is significant at 1 MHz in a standard buck converter.

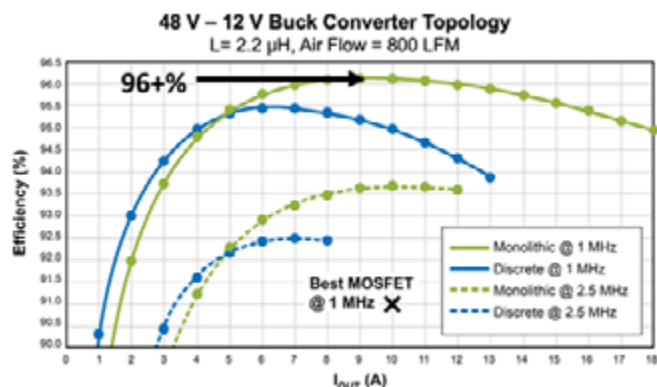


Figure 8: Efficiency comparison between the monolithic GaN power stage (green) and the externally-driven equivalent discrete GaN transistors (blue) solution in a 48 V – 12 V buck converter at 1 MHz (solid lines) and 2.5 MHz (dashed lines). The black "X" is the best reported MOSFET performance at 1 MHz.

Summary

An efficient circuit layout will minimize PCB area, reduce wasteful power dissipation due to slower switching speeds that are limited by parasitic inductances, and improve system reliability due to reduced voltage overshoot. Layout parasitics that are important when using GaN transistors were discussed; namely the common-source inductance, the high-frequency power loop inductance, and the gate loop inductance.

Several methods to minimize these performance inhibiting parasitics were reviewed, starting with the most basic single transistor through a complete monolithic GaN power stage IC. In future articles layout techniques discussed in this article will be built upon to show optimal thermal management systems design and how to create low EMI systems, all with modern chip-scale GaN transistors and ICs.

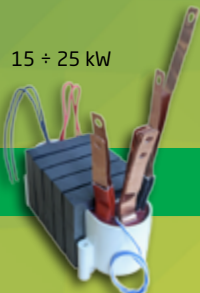
References

1. A. Lidow, M. de Rooij, J. Strydom, D. Reusch, and J. Glaser, GaN Transistors for Efficient Power Conversion, 3rd Edition, J. Wiley 2020.
2. Zhou, L., Wu., Y.F., and Mishra, U. (2013) "True-bridgeless totem-pole PFC based on GaN HEMTs," PCIM Europe 2013, pp. 1017–1022.
3. Efficient Power Conversion Corporation, "eGaN FETs in high performance DC-DC conversion," EDN Innovation Awards Conference and Awards, Shanghai, China, 2011, p. 28. Available from http://epc-co.com/epc/documents/presentations/EDN_Innovation_Conference_120111.pdf.
4. Direct Energy, Inc., "The destructive effects of Kelvin leaded packages in high speed, high frequency operation," Fort Collins, Colorado, Tech Note 9200-0002-1, 1998. Available from www.directenergy.com/index.php?option=com_joomdoc&task=document.download&path=ixysrf%2Fapplication-notes%2Fthe-destructive-effects-of-kelvin-leaded-packages-in-high-speed-high-frequency-operation.
5. Krausse, G.J. "DE-Series fast power MOSFET, an introduction," Directed Energy, Inc., Fort Collins, Colorado, Tech Note 9300-002 Rev 3, 2002. Available from www.directedenergy.com/index.php?option=com_joomdoc&task=document.download&path=ixysrf%2Fapplication-notes%2Fde-series-fast-power-mosfet.
6. Reusch, D. and Strydom, J. (16–21 March 2013) "Understanding the effect of PCB layout on circuit performance in a high frequency gallium nitride based point of load converter," OT Twenty-Eighth Annual IEEE Applied Power Electronics Conference and Exposition (APEC), Long Beach, CA, pp. 649–655.
7. A. Lidow, "The Ascent of GaN – Redefining Power Conversion with Gallium Nitride Integrated Circuits," Bodo's Power Systems, October 2020.

www.epc-co.com

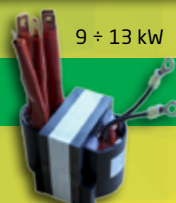
POWER TRANSFORMERS for HIGH FREQUENCY CONVERTERS

15 ÷ 25 kW




10 ÷ 16 kW

9 ÷ 13 kW

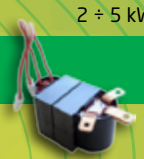


6 ÷ 12 kW


4 ÷ 8 kW



2 ÷ 5 kW



FULLY AUTOMATED JUST-IN-TIME PRODUCTION - MADE IN EUROPE



SIRIO
Inductive
Components

INDUCTIVE COMPONENTS
FOR HF INDUSTRIAL APPLICATIONS

SIRIO ELETTRONICA S.r.l.
Via Selve, 2 - 35037 TEOLIO (PD) - ITALY
Phone: 0039 049 9901090
Fax: 0039 049 9901868
E-mail: postoffice@sirio-ic.com
www.sirio-ic.com

45th ANNIVERSARY

For standard components visit
www.sirio-ic.com

1200 V Discrete SiC MOSFETs in a Comparison with the HighSpeed 3 IGBTs for Servo-Drive Systems

For applications like servo drives, size and weight are very important, however, cooling capability is limited. For this reason, discrete CoolSiC™ MOSFETs are the ideal solution for fulfilling these requirements and improving performance. The reduced losses allow for the implementation of a zero-maintenance fanless design. In addition, the motor and drive can be integrated, and therefore reduce the control cabinet size, and simplify cabling.

By Blaž Klobučar and Dr. Zhihui Yuan, Infineon Technologies AG, Austria

CoolSiC™ MOSFET in servo drives

One of the applications impacted by CoolSiC™ MOSFET performance are servo-drive systems, which are typically characterized by efficient, compact inverters such as those used in industrial robots and automation. Conduction and switching loss reductions can be obtained in all operation modes including acceleration, constant speed and braking mode.

Using CoolSiC™ MOSFETs in servo drives offers the following benefits:

- High acceleration and braking torque, which are key servo-drive parameters
- High reliability, low maintenance due to fanless drive solution

CoolSiC™ MOSFETs in servo drives also enable the integration of motor and drive, which means:

- There is only one cable from the control cabinet, which reduces costs by simplifying the connection, and increases system reliability due to fewer cables/less complex cabling
- There is no control inverter cabinet needed (or a smaller one only)

Servo-drive applications operate typically $\geq 90\%$ in a constant speed period with low torque, i.e. low current. In the acceleration and braking mode, the drive normally operates at a much higher current range. Here the dynamic loss could be reduced up to 50% compared with a Si IGBT, even at a low switching speed (5 kV/ μ s).

1200 V discrete Si IGBT vs SiC MOSFET

With respect to existing Si IGBT solutions, CoolSiC™ MOSFETs offer many reasons for providing the best performance in a variety of applications. For conduction loss, CoolSiC™ MOSFETs have resistive behavior, which results in a conduction loss reduction of up to 80% compared to IGBTs at a low current range. This greatly reduces the total system loss, since servo drives operate $>90\%$ of time at a relatively low current. 1200 V CoolSiC™ MOSFETs in power converters achieve much lower dynamic losses in comparison with Si IGBTs.

This is due to the unipolar structure of a MOSFET, where no minority charge carriers are involved during switching processes. Switching losses of CoolSiC™ MOSFETs do not increase with the temperature, which is what occurs with IGBTs.

Switching waveforms

Furthermore, the CoolSiC™ MOSFET does not need a co-pack diode; it uses an internal body diode that operates as a freewheeling diode. Using a MOSFET internal body diode leads to a huge reduction of Q_{rr} compared to silicon co-pack freewheeling diodes. It has been proven that using CoolSiC™ MOSFETs instead of Si IGBTs can reduce the heat sink size by 63% [2] and weight up to 65% [3].

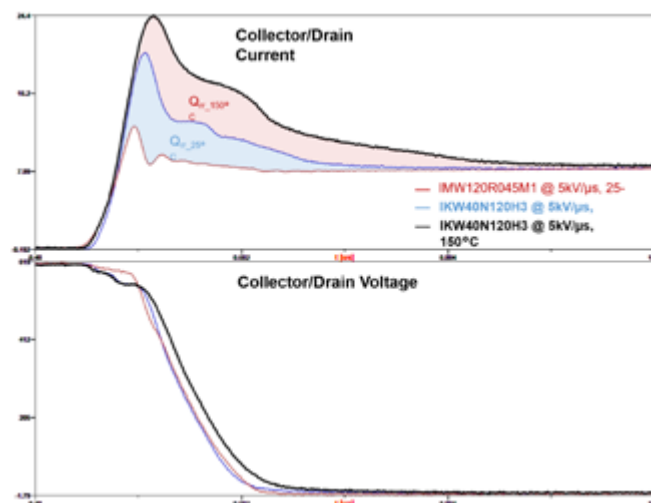


Figure 1: Turn-on switching behavior of Si IGBT vs CoolSiC™ MOSFET at 5 kV/ μ s

For applications such as servomotors and industrial robotic arms, where cooling capability is limited and efficiency important, using CoolSiC™ MOSFETs have huge advantages, especially if size, weight and compact design are key priorities for the system designer.

The long motor cables cause high peak voltages at the motor, which stress the motor isolation system and motor bearings. To protect the drive, manufacturers often stay under the 5 kV/ μ s switching speed. If a CoolSiC™ MOSFET is driven with low dv/dt, its switching losses will increase. However, the CoolSiC™ MOSFET still has more than 50% lower switching losses compared to high-speed IGBTs at 5 kV/ μ s.

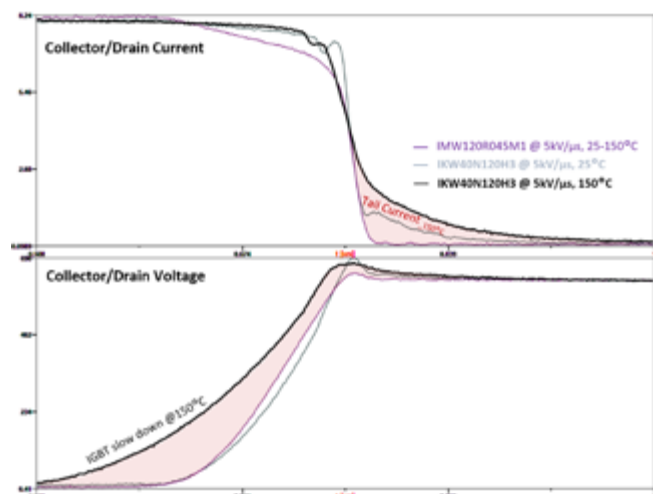


Figure 2: Turn-off switching behavior IGBT vs CoolSiC™ MOSFET at 5 kV/ μ s

In addition, CoolSiC™ MOSFETs have temperature-independent switching losses and smaller voltage overshoot, due to smoother current decrease. IGBT switching voltage has higher overshoot, and its switching speed slows down significantly at higher temperatures (see Figure 2). CoolSiC™ MOSFETs can switch with a speed exceeding 60 kV/ μ s, and there is a way to unleash the potential of the loss reductions. It can be done by implementing a dv/dt filter on the inverter output. In this way, the semiconductor can switch at maximum speed, and the filter will prevent the motor windings from stressing at high dv/dt and peak voltages. This has already been implemented in high-speed drives. In various studies, dv/dt filters have been presented with an improved filter solution that can be achieved by connecting the dv/dt filter to the middle potential of the DC-link. Using new motors with reinforced insulation systems together with minimized dv/dt filters are ways of making use of the full potential of SiC switches. [5]

Simulation and experimental validation

In order to see the performance of CoolSiC™ devices and understand the behavior of servo drives at different conditions, a simulation study was done, and compared with the experimental test results.

The junction temperature of the devices in a real system is very hard to measure, where normally the case temperature is detected. To have a more accurate estimation of a junction temperature, the simulation is recommended.

To finally confirm the performance of the proposed CoolSiC™ MOSFET discrete solution in comparison with the high-speed IGBT solution, a simulation model based on a three-phase B6 topology has been developed to estimate the junction T_j performance and corresponding losses of the inverter.

The results in Figure 3 show that even at 5 kV/ μ s, the strongly decelerated CoolSiC™ MOSFETs show up to 60% lower loss and 38% lower temperature rise of junction temperature (T_j) in comparison with the high-speed IGBT. This is due to the fact that body diodes have no (or very low) reverse recovery charge (Q_{rr}) and that CoolSiC™ MOSFETs have no tail current, as shown in Figures 1 and 2.

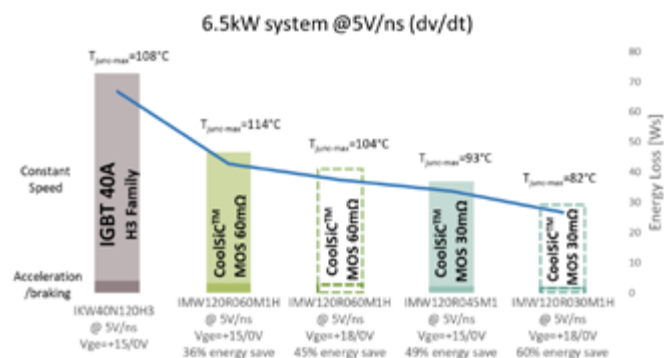


Figure 3: Thermal and loss comparison of CoolSiC™ MOSFET vs high-speed 3 IGBT for a 6.5 kW system at 5 kV/ μ s (dv/dt) switching speed for constant speed and acceleration/braking mode

New regulations [5] indicate that the switching speed of high-speed drives can be increased up to 8 kV/ μ s with 16 kHz switching frequency. Due to the much lower overshoot of CoolSiC™ MOSFETs compared to IGBTs, it is possible to run the CoolSiC™ in certain cases even higher. Servo-drive applications normally do not make use of long cables, which also enables faster switching.

When a CoolSiC™ MOSFET is driven with 8 kV/ μ s (instead of 5 kV/ μ s), up to 64% lower losses, and up to 47% lower temperature rise of the T_j , are possible in comparison with a high-speed 3 IGBT, which is shown in Figure 4.

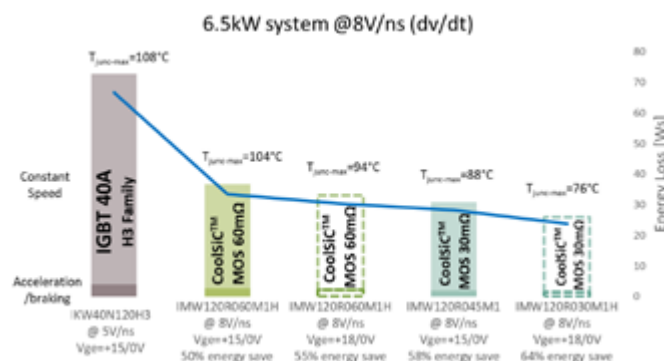


Figure 4: Thermal and loss comparison of CoolSiC™ MOSFET vs high-speed 3 IGBT for 6.5 kW system at 8 kV/ μ s (dv/dt) switching speed for constant speed and acceleration/braking mode.

Infineon CoolSiC™ MOSFET devices when driven with 15 V ($V_{gs,on}$), have a unique feature enabling short-circuit capability of 3 μ s under maximum ratings specified in the data sheet. To have a fair comparison with other SiC MOSFETs on the market, driving Infineon CoolSiC™ MOSFETs at a gate voltage ($V_{gs,on}$) of 18 V enables a power/current handling capability via lower $R_{DS(on)}$ (in this case a short-circuit capability is not available).

Conclusion

The test results and the simulation validation have confirmed that using CoolSiC™ MOSFETs in servo drives leads to 64% loss reduction and 47% lower temperature rise at low switching speeds (5-8 kV/ μ s).

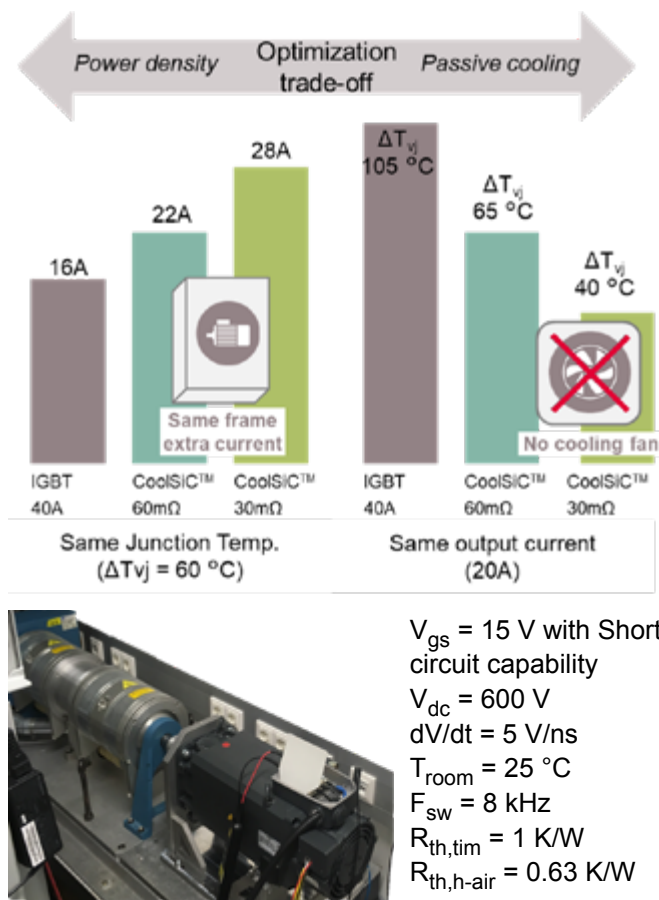


Figure 5: $R_{DS(on)}$ selection example for various target requirements of a servo-drive solution and motor test setup with test condition

By using a 60 mΩ CoolSiC™ MOSFET to replace the 40 A IGBT in a servo-drive application, while keeping the heat sink and dv/dt requirement, the total semiconductor loss drops by almost half at similar maximum junction temperatures.

CoolSiC loss reduction provides a new degree of flexibility for system improvements:

- Trade-off between output current, T_j , cooling efforts and $R_{DS(on)}$ selection
- The low ΔT_j from CoolSiC™ MOSFETs enables passive cooling

References:

- [1] Dr. Fanny Björk, Dr. Zhihui Yuan Infineon Technologies AG, Austria. CoolSiC™ SiC MOSFETs: a solution for bridge topologies in three-phase power conversion 2019
- [2] Sahan Benjamin, Brodt Anastasia Infineon Technologies AG, Germany. Enhancing power density and efficiency of variable speed drives with 1200V SiC T-MOSFET. PCIM Europe 2017, 16 – 18 May 2017, Nuremberg, Germany
- [3] Tiefu Zhao, Jun Wang, Alex Q. Huang, Comparisons of SiC MOSFET and Si IGBT Based Motor Drive Systems 2007
- [4] S. Tiwari, O.M. Midtgard, T. M. Undeland. SiC MOSFETs for Future Motor Drive Applications 2016
- [5] K. Vogel, A. Brodt, A. Rossa "Improve the efficiency in AC-Drives: New semiconductor solutions and their challenges", EEMODS 2015
- [6] Eval-M5-IMZ120R-SiC <https://www.infineon.com/cms/de/product/evaluation-boards/eval-m5-imz120r-sic/>

www.infineon.com

pcim
EUROPE

International Exhibition and Conference
for Power Electronics, Intelligent Motion,
Renewable Energy and Energy Management

Nuremberg, 4 – 6 May 2021

Focused on
POWER ELECTRONICS?

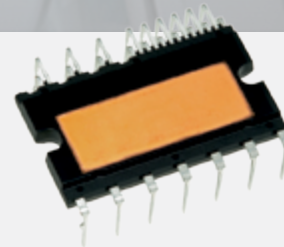
Exhibit at the PCIM Europe!
pcim-europe.com/exhibitors

One of our
key products:
Trust.

Power Devices from Mitsubishi Electric.

Home appliances are becoming more and more demanding regarding functionality, reliability and efficiency. In the field of Power Semiconductors Mitsubishi Electric had created the necessary basis over 20 years ago as the pioneer of the DIPIPM™ transfer molded package intelligent power modules, followed by the continuous development and expansion of this series. Consequently, with the new SLIMDIP™-W a new Intelligent Power Module in the well-established SLIMDIP™ package has been added to the line-up to enable low losses with high switching frequencies, while keeping the electromagnetic noise low. The versatile integrated features give, for various applications in the industry and residential field, the benefit of reduced development time for the complete inverter system.

**New IPM in SLIMDIP™
package with latest RC-IGBT
chip technology**



The high-switching speed SLIMDIP™-W

- Optimized terminal layout enabling simple and compact PCB design
- Integrated driver ICs (HVIC and LVIC)
- Integrated bootstrap diodes and capacitors
- Short circuit protection through external shunt resistor
- Power supply under-voltage protection: Fo output on N-side
- Over temperature protection
- Analog temperature voltage signal output
- Low electromagnetic emissions



for a greener tomorrow

More Information:
semis.info@meg.mee.com
www.mitsubishichips.eu



Scan and learn more about
our Power Semiconductors
on YouTube.

**MITSUBISHI
ELECTRIC**
Changes for the Better

Enabling High Temperature Operation of Optimized DC Link Capacitor/Bus Test Kit

Combination of Kaladex® PEN HV™ dielectric by DUPONT TEIJIN FILMS and wound by ADVANCED CONVERSION, integrated into the DC link, enables power dense high switching frequency inverters with superior current rating.

*By M. A. Brubaker and E. D. Sawyer, Advanced Conversion
L. Schosseler, DuPont Teijin Films (DTF)*

Introduction

DuPont Teijin Films (DTF) is a global manufacturer of polyester films with applications in very diverse domains. DTF introduced the Kaladex® PEN HV™ dielectric in 2016 and the technology of capacitors based on this new dielectric is already commercialized or in development. The Kaladex® PEN HV™ dielectric film combines the high temperature capability of PEN films ($> 125^{\circ}\text{C}$) with outstanding electrical break-down strength and self-healing properties comparable to polypropylene [1]. This unique property set allows Kaladex® PEN HV™ to support higher hotspot temperatures for advanced DC link capacitors needed to enable fast switching, power dense inverters. Existing DC link designs can now achieve a higher current rating with no other changes to the customer system, or the same current rating can be held with a significant reduction in the cooling infrastructure to save cost, weight, and volume.

Advanced Conversion has successfully utilized Kaladex® PEN HV™ from DuPont Teijin Films in high performance DC link capacitors for a variety of electric vehicle and aerospace applications. This article has been written in response to assertions made by FTCAP in the April 2020 issue of Bodo's Power Systems that the Kaladex® PEN HV™ material is "unsuitable" for 125°C capacitor applications. We have performed ripple current testing on a standard capacitor/bus "test kits" that uses the PEN HV™ film to demonstrate excellent high temperature performance. High temperature stress testing has also been performed to show that the dielectric is stable.

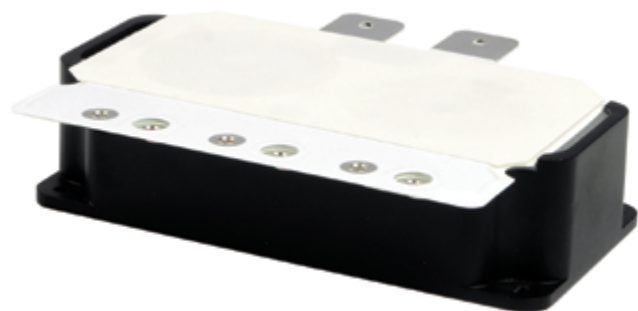


Figure 1: Advanced Conversion 906A107 capacitor/bus test kit (500V and 550µF) for the Infineon HybridPACK™ Drive module.

The 906A107 [2] is a standard DC link capacitor/bus test kit (500V and 550µF) using Kaladex® PEN HV™ film shown in Figure 1 that connects to the Infineon HybridPACK™ Drive module [3]. The polypropylene version of this DC link kit (700A186) has been described previously and demonstrated to enable the best possible performance for this switch module [4]. The low inductance properties of the 700A186 are preserved in the 906A107 using the same mechanical package, but an increased current rating is now possible since the Kaladex® PEN HV™ film can safely support a significantly higher hotspot temperature.

A 906A107 part was instrumented with type k thermocouples and installed between two temperature-controlled plates as illustrated in Figure 2 to mimic the thermal boundary conditions assumed for the datasheet rating curve. A 20kHz AC sinusoidal current source was connected to the capacitor with air-cooled copper conductors to minimize external heat input. The entire assembly was then insulated such the internal heat was removed dominantly through the top and bottom plates. The cooling plates were set to 90°C and two hours was allowed for the setup to get close to equilibrium. At this point, a 175Arms ripple current was run through the capacitor assembly and the setup was run for an addition two hours to reach a stable thermal equilibrium.

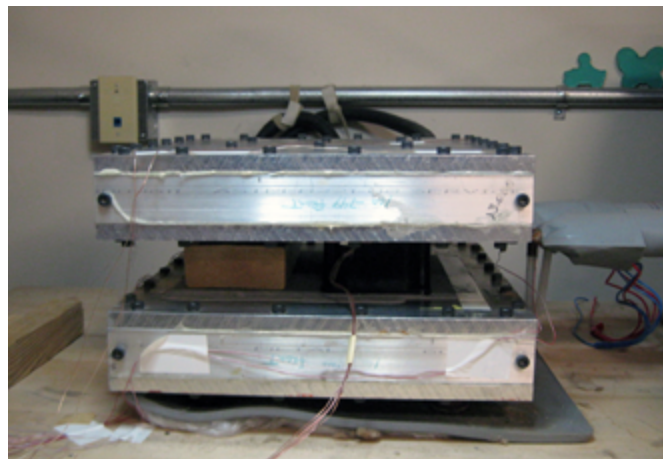


Figure 2: The instrumented 906A107 capacitor bus installed between temperature-controlled plates for high current testing.

Test Results

The capacitor winding core temperature which corresponds to the winding hotspot is presented along with the top and bottom plate temperatures over the duration of the experiment in Figure 3. As shown in the graph, the thermal time constant is about 30 minutes, and the hotspot temperature stabilizes at 130°C. Consider the rating curve for the 906A107 as shown in Figure 4 which assumes similar thermal boundary conditions to the test setup. The rating curve indicates a 180Arms current rating at 90°C case temperature which is based on a 130°C hotspot, which agrees to better than 3% with the data of Figure 3. Note that the rating for the polypropylene version of the test kit is also shown on Figure 4, which indicates the Kaladex® PEN HV™ film enables a rating increase of 75% with a 130°C hotspot.

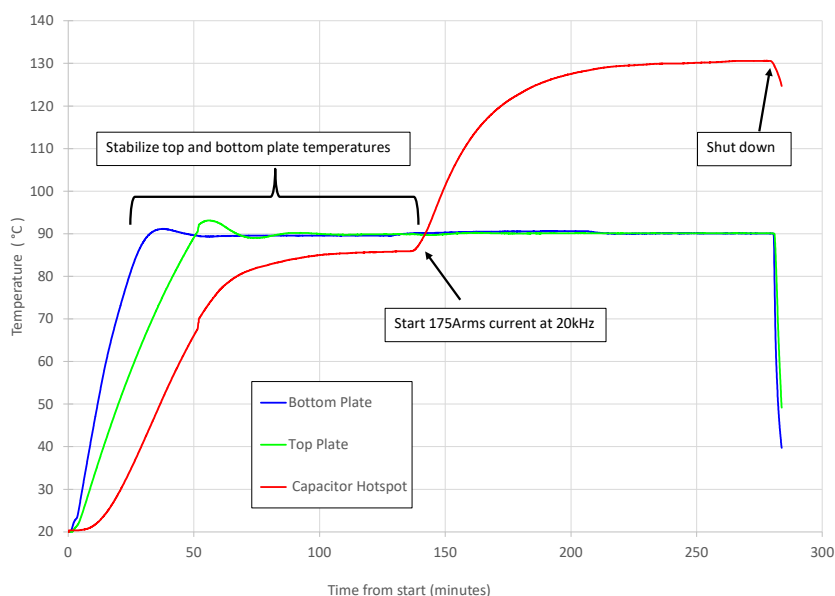


Figure 3: Temperature rise testing results with 90°C boundary temperature and 175Arms ripple current at 20kHz.

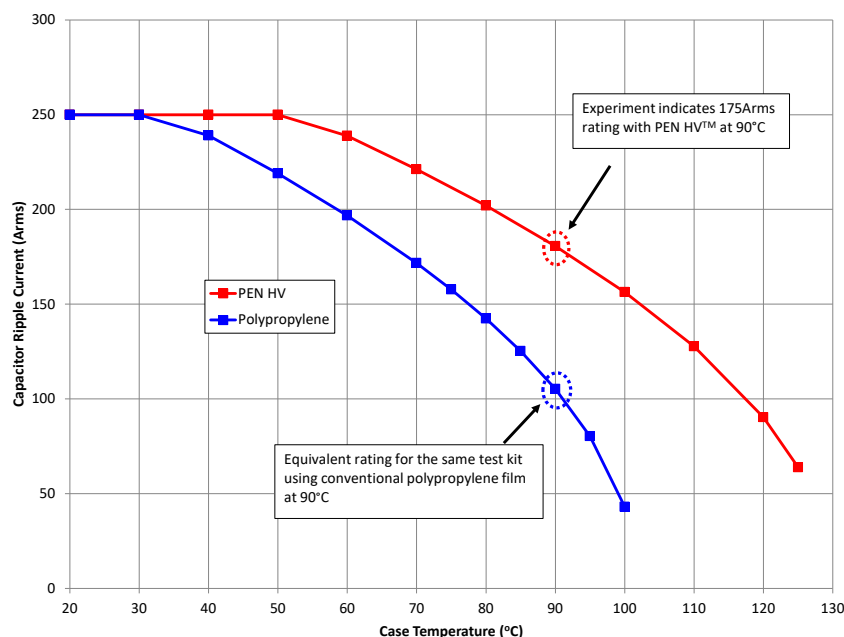


Figure 4: Rating curve for 907A107 test kit showing increase enabled by PEN HV™ over conventional polypropylene.

Additional testing was undertaken to demonstrate stability of the Kaladex® PEN HV™ subject to temperature and voltage stress. Test parts were stressed at 25°C and rated voltage, 85°C and rated voltage, and 130°C with the voltage re-rated linearly above 125°C. In each case, the parts were soaked for over 1 hour to achieve full thermal equilibrium. Note that the datasheet for the 906A107 indicates derating to 460V at 130°C for the stress test, which is calculated based on assuming a linear decrease from 500V to 300V as the temperature is increased from 125°C to 150°C. Many high temperature films suffer from excessive DC leakage current at elevated temperature which can create a thermal runaway scenario. The Kaladex® PEN HV™ dielectric does not exhibit any stability or DC leakage issues at these stress levels and we have not seen any problems in the field.

Conclusion

Advanced Conversion has provided further validation of the DuPont Teijin Films Kaladex® PEN HV™ material for high temperature capacitor applications using a 906A107 capacitor/bus DC link test kit. The capacitor was made using our proprietary winding and packaging technology which has been repeatedly demonstrated to work well with the Kaladex® PEN HV™ material. The test kit was successfully run up to 130°C hotspot temperature using a 175Arms ripple current and the capacitor film functions with 460V applied at this temperature without any problems.

This validates the scaling of the entire rating curve which is based on a 130°C hotspot temperature limit as a function of case temperature. We have multiple customers using parts made with PEN HV™ and we have not seen any field failures to date. As such, we respectfully disagree with the assertion by FTCAP that this material is not suitable for high temperature capacitor applications.

References

- [1] L. Schosseler, "A new commercial High Temperature Capacitor Dielectric for Power Applications", Bodo's Power Systems, April 2016.
- [2] Advanced Conversion 906A107 datasheet: https://advanced-conversion.com/wp-content/uploads/2020/05/power_ring_906A107_web.pdf
- [3] Infineon, "Compact Power Modules", Electric & Hybrid Vehicle Technology International, July 2014.
- [4] M. A. Brubaker, T. A. Hosking, T. Reiter, M. S. Chinthavali, and L. D. Marlino, "Optimized DC Link for Next Generation IGBT Modules" Proceedings of PCIM 2016, Nuremberg, Germany, May 16-18, 2016.

Bidirectional Wireless EV Charging - Smart Grid Integration at Highest Comfort Level

The rate of electrification of the mobility in industries or transportation depends upon the deployment of the charging infrastructure. The existing solution, namely conductive charging, has several concerns in safety, robustness and comfort due to plugging-in of huge cables, especially for higher power. Wireless charging is touted to provide a safe, clean, and autonomous solution.

By Sri Vijay Vangapandu and Tobias Herrmann, Finepower

What is wireless and inductive power transfer (IPT)?

The scientist Nikola Tesla coined the term "Wireless Power Transfer" (WPT) and presented a contactless system in 1893. The fundamental principles that govern this technology are Lenz's law and Michael Faraday's law of induction. There are many methods by which this can be employed. The most successfully commercialized (at low power levels) is "Inductive Power Transfer" (IPT). IPT uses near-field technology where the energy remains within a small region of the transmitter.

Finepower develops solutions for wireless (inductive) power transfer since several years. Now we are extending this technology to bidirectional operation in conjunction with high power, low voltage batteries in the research project BiLiA which is funded by the Bavarian Ministry of Economics and project execution organization VDI-VDE-I.

IPT magnetic Coil System

The magnetic coupling stage is the most important part deciding the design of power electronics, efficiency, and transferable power. In a typical application as electric vehicle charging, the secondary side coil is attached on the bottom side of the vehicle. The primary coil side is put on the ground. This assembly is ensured to have flux in between those two coils by using ferrite and aluminum on the outer sides of each coil. Stacking or shaping of the ferrite blocks is also possible. The airgap between the coils can be quite large, depending upon the vehicle's ground clearance. This leads to leakage inductance of similar dimensions as the mutual inductance. Each coil in the IPT system can have circular, rectangular, solenoid, DD, DDQ, bipolar, etc. shapes. The

advantages of each coil system vary across interoperability, size, flux leakage, positional tolerances, and operational complexity. At higher powers, to reduce the ampere-turns (or Magnetomotive force) a bifilar winding is used. The efficiency of the entire IPT system is limited by the native quality factor of the coils. This can be increased by using a Litz wire carefully reducing the skin and proximity losses at both bundle and strand level.

Optimizing the resonant circuit maximizes efficiency

The simplified model of a typical inductive charging system is shown in Figure 1. A high frequency (i.e., 80-90 kHz) inverter after a PFC converts the rectified grid voltage into an AC square wave which is necessary for effective power transfer.

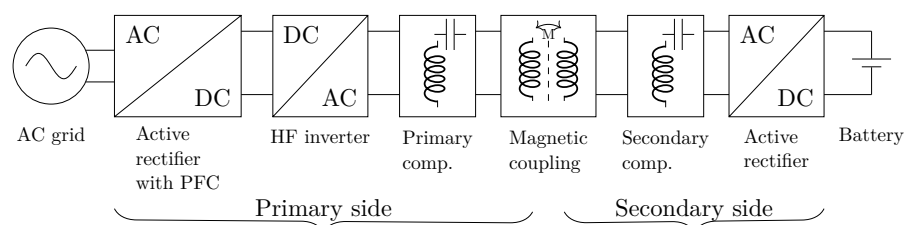


Figure 1: Block diagram of a typical inductive charging station. Grid power is rectified and converted to a high-frequency signal using PFC and inverter, respectively. This high frequency current signal through the primary coil generates a flux. Thereby, inducing a voltage across the secondary. The signal is later rectified to deliver power to a DC battery load.

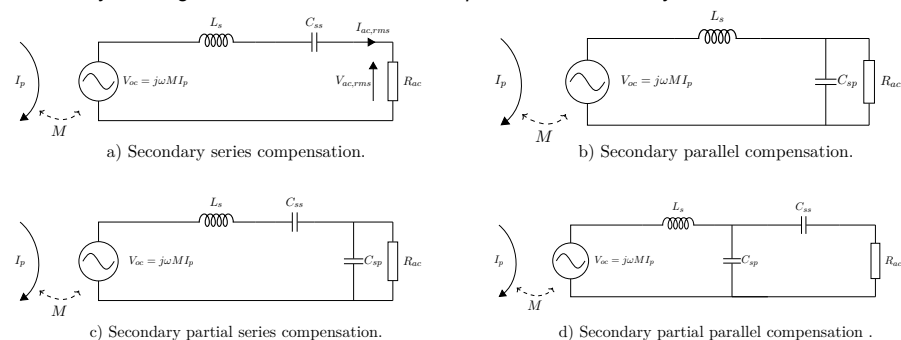


Figure 2:

a) On the secondary side, a series capacitor C_{ss} is added. A properly chosen value can cancel the secondary inductance (ωL_s) to improve the power transfer. The impedance seen by V_{oc} is purely resistive at this frequency. This is typically used in constant voltage applications.
b) A parallel capacitor replacing the series one is useful in constant current applications.
c+d) Hybrid compensation type where the series and parallel capacitors can be adjusted are also possible.



HITACHI **ABB**

HITACHI ABB POWER GRIDS

IGCT HIGHEST POWER DENSITY FOR MOST COMPACT EQUIPMENT

The IGCT is the semiconductor of choice for demanding high-power applications such as wind power converters, medium-voltage drives, pumped hydro, marine drives, co-generation, interties and FACTS. Hitachi ABB Power Grids' range of 4500 to 6500 volt asymmetric and reverse conducting IGCTs deliver highest power density and reliability together with low on-state losses.



This high frequency current through the primary coil generates a flux inducing a voltage across the secondary side. This voltage is called open-circuit voltage (V_{oc}), given by Equation 1 where I_p is the primary coil current, M is the mutual inductance and, ω is the angular frequency.

$$V_{oc} = j\omega MI_p \quad (1)$$

V_{oc} , when connected to a load delivers power and is given by Equation 2 where R_{ac} is the equivalent load resistance (The impedance presented by the active rectifier and load to the secondary side.) L_s is the secondary inductance.

$$P_{out} = \frac{V_{oc}^2 R_{ac}}{R_{ac}^2 + (\omega^2 L_s^2)} \quad (2)$$

Using maximum power transfer theorem with Equation 2, the maximum output power is achieved at $R_{ac} = \omega L_s$. Adding a series capacitor in the equation with $1/\omega C_s$ to cancel the term ωL_s can double the maximum transferable power. But instead of a series, different other compensation topologies are also possible. They can be any T (or π)-network built using passive energy storage components. Some simplified tuning networks on the secondary side are shown in Figure 2.

The output power of the circuit can also be written as in Equation 3, where I_{sc} is the current on the secondary side under short circuit condition and Q_2 is the secondary load quality factor.

$$P_{out} = V_{oc} I_{sc} Q_2 = \frac{\omega M^2}{L_s} I_p^2 Q_2 \quad (3)$$

From the Equation 3, the primary coil current can be reduced by increasing Q_2 and thus, reduces the losses. But the bandwidth of the system will be reduced, making the implementation of the control system more difficult. The required volt-ampere rating of the secondary coil also increases.

The primary side inductance is compensated to achieve a phase lag of the inverter current to the voltage thereby enabling zero voltage (and/or zero current) switching of the power transistors. This improves the system efficiency significantly. Capacitance values are chosen to resonate with the respective coil inductances for a simple series-series (S-S) compensation.

Bidirectional power flow reduces grid costs

To reduce greenhouse-gas emissions, there is a strong push towards renewable energies. Most prominently solar and wind power.

But sunlight and wind flows are intermittent and such fluctuations can destabilize the grid. Also, in the pursuit of energy independence, many industries are installing their own systems. This is due to increasingly ease of access to renewable energy technologies. For instance, car fleet owners, driven to electrify their vehicles would benefit from the (cheaper) generation of their own power and therefore install grid systems or charging points. On the other hand, this could lead to an increasing need of large land space to cover peak power demands. Smart grid storage systems, however, can reduce the required peak power. By storing energy during peak availability and supplying it when needed, the power flow can be managed and external demand from the grid can be stabilized.

Due to relatively large capacities, electric vehicle batteries can be viewed as ideal energy storage elements for grid stabilization. Therefore, battery chargers, including wireless systems, should be enhanced to provide bidirectional operation.

A modified model of the IPT system with bidirectional functionality is shown in Figure

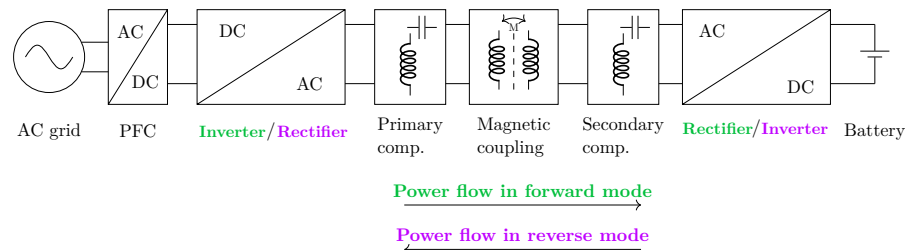


Figure 3: The system is like in Figure 1, but with dual operation possible for both DC-AC and AC-DC converters. This allows bidirectional power transfer.

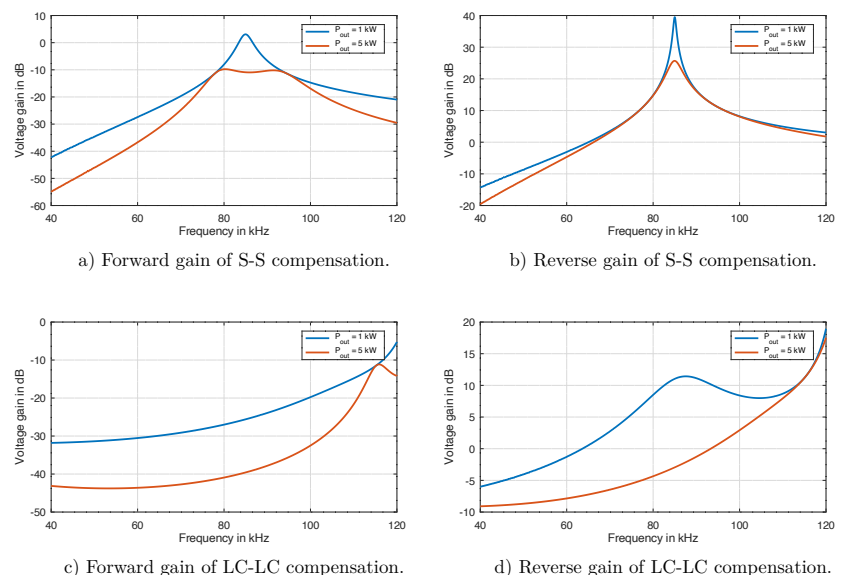


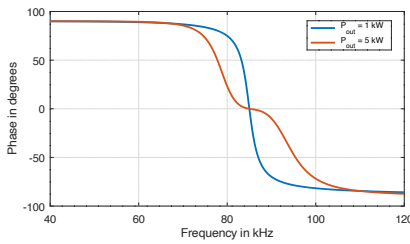
Figure 4: AC gain response in both the power flow directions are plotted for S-S and LC-LC compensations. Both are tuned to operate at 85 kHz.

3 In the forward mode, power flows from the grid to a battery load. The block after the PFC acts as an inverter exciting the primary coil. A rectifier is required to convert the AC power from the secondary coil to a battery. The respective functions of these blocks will be interchanged, while in reverse mode. The choice of the compensation type and its values depend upon many criteria. Some of them are discussed below:

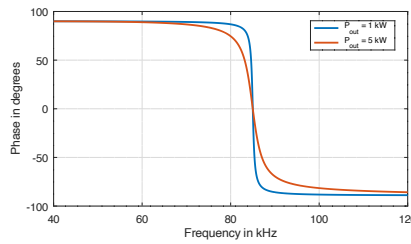
Controllability: The common control method is the primary control. This method controls the high frequency (HF) inverter output voltage as the primary coil input voltage. According to the Equation 4 either voltage control or phase control is possible. Where V_{dc} is the PFC output voltage and α is the phase angle.

$$V_{in,rms} = \frac{2\sqrt{2}}{\pi} V_{dc} \cos \frac{\alpha}{2} \quad (4)$$

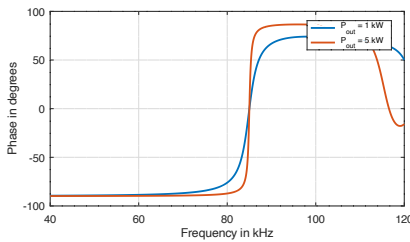
Typical voltage transfer functions of a S(erial)-S(erial) and LC-LC compensation are shown in Figure 4. The coil position is fixed delivering 1 kW and 5 kW. The plots show the functions in both forward and reverse modes. The load quality factor should not be too high, otherwise, the required



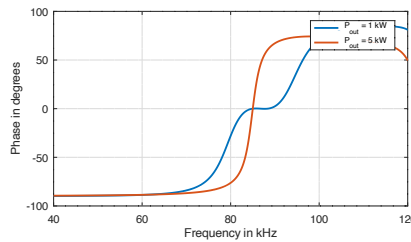
a) Forward input phase of S-S compensation.



b) Reverse input phase of S-S compensation.



c) Forward input phase of LC-LC compensation.



d) Reverse input phase of LC-LC compensation.

Figure 5: Input phase response to check for ZVS operation possibility in both the power modes

operating range can exceed the specification of the inverter. On the other hand, a low quality factor will not fully utilize the available operating range. As can be seen in LC-LC compensated gain response, the variation of the gain is low. And in S-S forward response, pole splitting happens at higher powers. This complicates the design of the control system.

The corresponding input phase responses are plotted in Figure 5. The phase response starts flattening (across the operating range) in the S-S forward, limiting the available ZVS range. Whereas in reverse mode, the sharp changes due to high quality factors demands a lot of reactive power. The same trend can be observed in LC-LC, but with interchanged responses.

Simplicity: By extending LC to the partial-series topology LCC, the quality factor can be improved which suits the primary control. But it increases the cost and complexity due to the added components. Also using the same type of compensation on both the sides maintain symmetry and can reduce the design efforts.

Reflected impedance: The reactive component of the reflected impedance effects resonance. In partial-parallel compensation, there is always some reactive component. Whereas both the S-S and LCC-LCC compensation would have zero reflected reactance when operated below resonance (except if there is an offset between the coils). If care is not taken, this can limit the soft turn-on of the transistors in some scenarios, thus reducing the operational efficiency. Adaptive tuning can help in alleviating this issue. With proper

design techniques, an optimal choice of tuning can be obtained to ensure ZVS operation in both modes across positions.

To sum it up, it is necessary to consider all the constraints for both forward and backward operating modes from the design start of a bidirectional wireless charging system. The performance will degrade if the coil parameters and tuning system are selected in the same way as for a unidirectional design. Therefore, a bottom-up approach is needed to compile all requirements and constraints from the beginning to optimize the magnetic system while considering the cost and limitations on the power electronics.

Finepower is continuously extending the technical limitations of wireless charging and supports customers to efficiently implement this technology into their respective applications.

About the authors

Main author:

Sri Vijay Vangapandu received master's degree at the Technical University of Munich in 2019. He works in the field of inductive charging for industrial and automotive applications at Finepower GmbH in Ismaning/Munich.

Co-Author:

As Field Application Engineer and Marketing Manager, Dipl.-Ing Tobias Herrmann is responsible for both the technical support of customers, as well as the technical and visual marketing activities of Finepower.

www.finepower.com

January 2021

www.bodospower.com

MUE CAP

CAPACITORS

- DC-CAPACITORS
- AC-CAPACITORS
- PULSE-CAPACITORS
- RESONANT-CAPACITORS

LUG-FILM



- Lug design adapted to individual IGBT
- High du/dt
- 250Vdc - 3000Vdc

RADIAL FILM



- Custom Design
- Up to 6 Pins
- Harsh environment protection available

AXIAL-FILM



- Polypropylen / Polyester
- 63Vdc - 10.000Vdc
- Flat & zylindric Design

info@muecap.de

www.muecap.de

3D Bond Wire Modelling and Electro-Magnetic Simulation Accelerates IGBT Module Development

Speeding up the electro-magnetic module design for maximum Chip performance utilization and highest robustness with latest tools for bond wire routing and electromagnetic simulations.

By Raffael Schnell, SwissSEM Technologies AG and Samuel Hartmann, MFis GmbH

Creating bond wire layouts using 3D CAD

Although 3D CAD systems today are well established in power module development for virtual prototyping and creation of the necessary product documentation, the bond wires are often missing in 3D models. While a single bond wire can be modelled with some arcs and lines, modelling a whole bond wire layout is time consuming, since often each bond wire has its individual geometry. To fill this gap, the first version of the software MFis Wire was released in 2020 by MFis GmbH, a company providing engineering services and tools with a focus on power electronics packaging.

MFis Wire provides a user-friendly interface (see figure 1) and makes 3D modelling of wedge, ribbon, and ball bond wires fast. A bond wire is drawn by selecting start and end point of the wire and interactively defining its loop shape and foot rotation. Many CAD commands like copy, move, mirror, array can be used to modify one or more selected bond wires or bond points for example for adjusting the pitch of a row of bond wires.

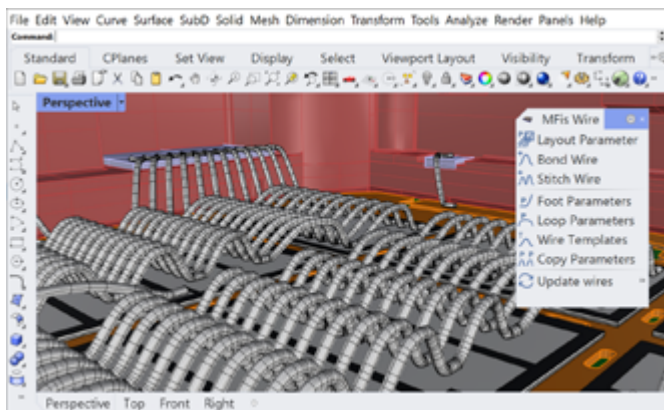


Figure 1: The software MFis Wire, used for drafting the bond wire layout of the ED-type power module

The software has been realized as a plug-in for the powerful and affordable Rhino3D CAD platform. For creation of bond wire layouts only basic skills of CAD modelling are needed. Short training videos showing the workflow guide the user to create first wire layouts within short time. Once a 3D model is ready, it can be exported to many industry standard CAD formats or converted to a 2D drawing with bond

point coordinates. Since Rhino3D has powerful rendering features, photo-realistic images of a power module layout are created with low effort (see figure 4).

Geometry optimization for fast parasitic extraction

A 3D bond wire layout geometry can for example be used for documentation, electro-thermal finite element analysis or parasitic extraction purposes. Depending on the targeted use, the wire cross sectional geometry must be chosen differently. For documentation purposes a circular cross section looks most natural and has lowest file size.

When targeting electro-thermal finite element analysis, only the cross-sectional area of a wire is of relevance. The best choice is a triangular cross-section with the same cross-sectional area as the original wire, which makes the geometry efficient for meshing and computation and will not influence the bond wire temperatures and resistances obtained as a result from the finite element analysis.

For parasitic extraction, the cross-sectional shape is relevant. If circular cross section is used, the mesher of the parasitic extractor will approximate the round shape with several elements. Typically, a better trade-off between computing time and accuracy is achieved when the approximation is already implemented in the input geometry. Good results are obtained using a hexagonal wire cross section.

Bond wire geometry modelling and parasitic extraction was done for the ED-type module with a bond wire layout consisting of 165 wires, many of them having their individual shape. After having created the wire layout, that connects 661 points, the wires were exported in variants with circular and hexagonal cross sections and processed using the parasitic extractor Ansys Q3D. Figure 2 shows the difference in mesh obtained for the variants with circular and hexagonal cross section. For the wire with a circular cross section the mesher puts a lot of triangular cells to approximate the round shape, which resulted in most realistic results, but needed 5.5 hours to converge in contrast to only 71 minutes in case of the geometry with hexagonal cross section. Also, the memory consumption of 22.3 GB was much higher for circular wires than 11.4 GB for hexagonal wires. The difference in the obtained module self-inductance was only 0.1 %.

ED-Type module design optimization

As an emerging company it is crucial for SwissSEM Technologies AG to bring its first products to the market in high quality and short time. Electromagnetic and thermal optimization are essential for excellent device performance. The ED-Type, an industry standard 17 mm height 62 x 152 mm IGBT module, offers special challenges for internal current sharing between the IGBTs due to its longish design. Most classic layouts suffer more or less current imbalance between the chips, and it is our goal to launch a module with the best possible current homogeneity in order to have the full benefit of our latest IGBT i20 generation.

With the help of the MFis Wire software we were able to quickly generate various design variants including variations in the bond wire layout. This enabled us to simulate the electromagnetic couplings of the variants in Q3D and make switching simulations with the SIMetrix Spice simulator using the extracted circuit models from Q3D. These simulations were the basis for a better understanding of the device and its internal couplings. Especially as already small variations of

the wire position and shape in the mm range can have a significant impact on the coupling. Hence a simplified geometry, as it would be obtained when using the wire tool available in Q3D, is not sufficient. Together with heat-transfer simulations an optimized layout was found. From thermal resistance point of view both variants of chip positioning offer the same R_{th} . However, the "Layout straight" offers more potential to improve the current sharing compared to the "Layout classic", especially to slow down IGBT #3 which is closest to common power emitter connection (see figure 3). For the final layout optimization, the gate-position of IGBT #3 was rotated and the main emitter wire and gate wire layout was optimized (see figure 4). As a result, the current imbalance was reduced from 30% of the "Classic layout" to 17% of the "Layout straight optimized". This is a significant step that improves the load balancing within the IGBTs, but as well yields in a higher safe operating area utilization of the IGBT chips.

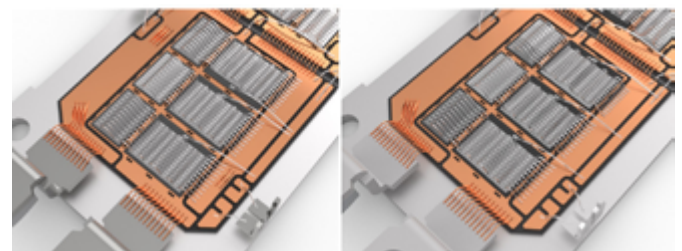


Figure 4: Layout straight (left) – Layout straight optimized (right)

Conclusion

Today's simulation tools for thermal as well as electro-magnetic simulations are very powerful, shorten development time and improve the quality of IGBT module designs significantly. Still the input for the finite element simulations need to be as accurate as possible and reflect the final product design if the optimal result is to be achieved. Especially for complex details like wire bonds, obvious simplifications are attractive at first glance due to the tedious and time-consuming work it requires in the CAD. However, the accuracy of the results will suffer from simplifications, and the full potential of the simulation tools is not utilized.

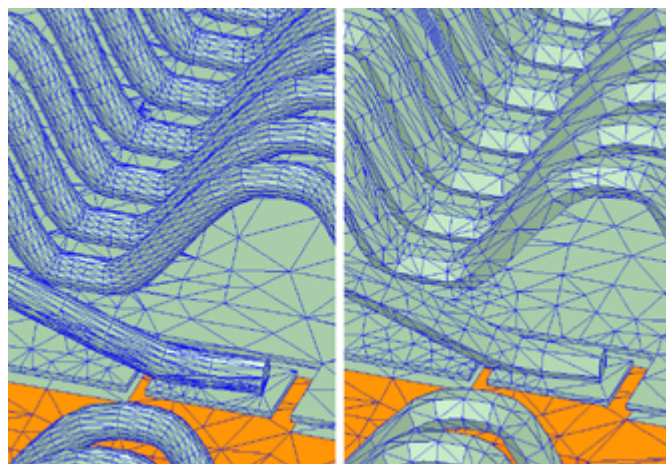
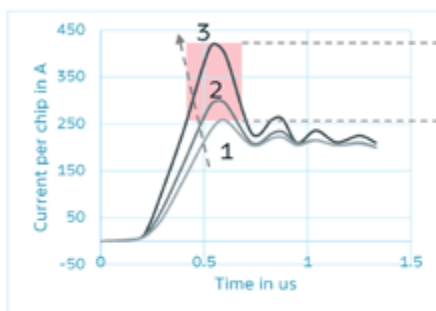
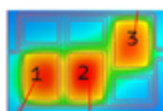


Figure 2: Mesh created by Ansys Q3D for bond wires with circular and hexagonal cross sections

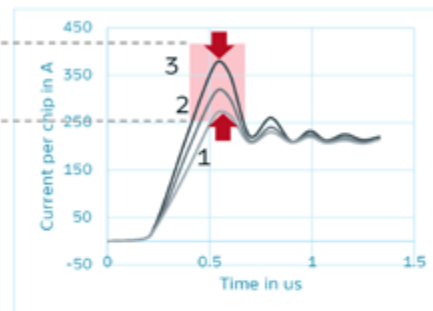
Layout classic



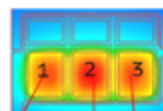
30% imbalance in turn-on current



Layout straight optimized



17% imbalance in turn-on current



By using the software MFis Wire, time is significantly shortened for creating complex 3D geometry models of bond wire layouts. Using hexagonal wire cross section in the input geometry of the parasitic extractor results in four times faster computation, which makes it possible to investigate several layout variants in a single workday. This method used at SwissSEM, enabled an improvement of the ED-Type module's internal current sharing by nearly a factor of two compared to classic design approaches.

www.swiss-sem.com

www.mfis.ch

Figure 3: Comparison of current sharing with different layouts and thermal reference

GaN Transistor Eliminates EMC at Source

EMI problems are often the last major bottleneck at the end of product development. Modelling and first measurements help to reduce the risk, but especially when a compact design is required, there is little space for last-minute changes. As time scales slip, the prices of the components used increases in proportion to the desperation and pressure to get the unit to market.

By Nigel Springett, Ing Büro Springett

The problems of EMI

I have rarely seen EMI filters being cost optimised once a solution has been found. Time, engineering budgets and risk do not allow it; making it even more important to have a good and cost effective EMI solution from the start. Recently I was helping to debug a 3kW single phase unit with a standard boost PFC. The transistor a standard 650V T0-247 super junction MOSFET was injecting lots of common-mode noise into the chassis. Eliminating the source of the noise by replacing the mosfet with a source tabbed, Nexperia GAN063-650W, was a simple and cost effective solution. This article shows measurements and diagnostic methods.

LISN

EMI measurements are conducted using a LISN at the power supply input. The LISN provides a defined source impedance for the measurements as well as removing low-frequency signals.

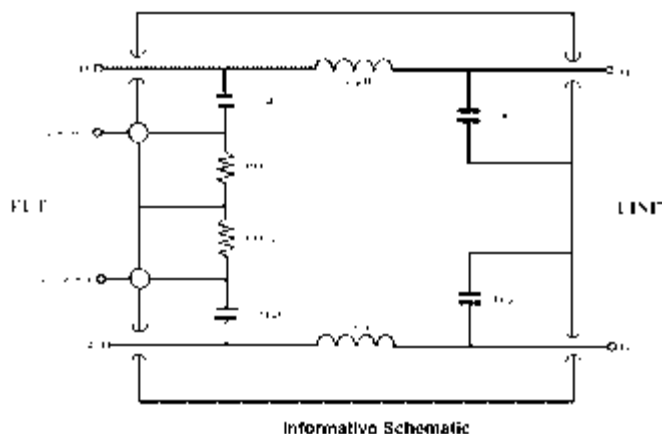


Figure 1: Standard LISN

Figure 1 shows the standard LISN. The 50Ω termination in the receiver with the 100nF cap, give an LF cut-off frequency of 30kHz; which effectively removes mains ripple from the measurement so the small level disturbances can be seen by the receiver. To look at the HF disturbance with a scope, it is necessary to remove the dominant mains. A 50Ω system as used in the LISN would change the system and significantly distort the measurements, so a high impedance filter (1nF cap with 10k to GND) was used. The filter removes the low frequency components. Only the HF noise is visible without significantly loading the circuit. The scope maths channel was used to calculate the differential part of the noise. (ch1-ch2) and to get a feeling in real-time how effective the filter is.

Measurements

Using the HF filter, the noise can be seen at various nodes around the PFC schematic (Figure 2). The overlaid green and yellow traces show the voltage to ground, and the light blue trace is the differential voltage. Note the scaling is 2V/div and 1V div for the maths channel.

Looking at the various plots; (5) the output, after the inductor has almost no common mode noise (blue). At the MOSFET (4), the common-mode noise can be clearly seen to be synchronised with the switching of the MOSFET. Plot 3 shows the noise that the filter should attenuate, common-mode noise is dominant, but also significant differential noise. Plot 2 shows the noise after one filter stage. The scaling is the same as plot 3, switching frequency common-mode noise has been reduced 14dB from ~1V to ~200mV; we could expect more from a filter stage.

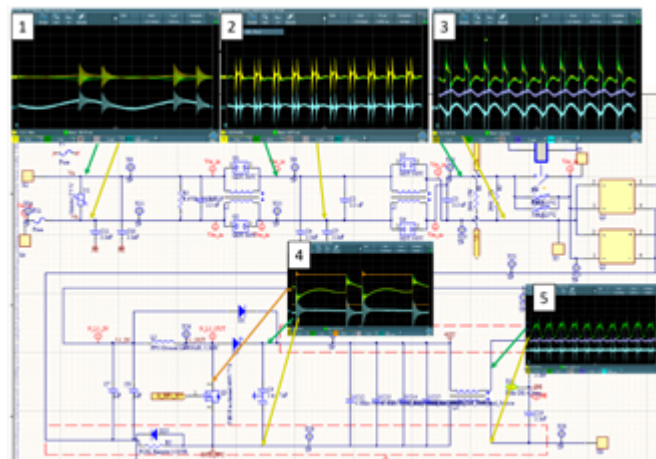


Figure 2: HF noise around the schematic

The plots clearly show noise is produced by the MOSFET (no great surprise!), but more surprisingly most of the high frequency noise is common-mode (plots 1-3). Removing the drain from the grounded heatsink confirmed that the capacitance of the MOSFET case, switching 400V in 20nS, generates most of the common mode noise.

Current injected into the heatsink

The MOSFET tab has an area of about 245mm². It is mounted on a 100μm isolator which creates a capacitance of around 120pF to the heatsink. At 20V/nS, the current injected into the heatsink is 400mA. The return part for this current is first the local Y caps. Ignoring

inductance; the voltage over the Y capacitors can be calculated as a voltage divider; tab capacitance with 120pF and 400V divided by the Y capacitors ($2 \times 4n7$), resulting in 5V (134dB μ V) over the Ycap (close to the measured value). To meet a 65dB μ V EMC limit; a filter with about 70dB attenuation would be required. As the Y capacitance value is limited due to earth leakage currents, only the inductance can be increased. A 2-stage filter with 65dB at 200kHz could have 10mF and 10nF Ycaps, which is large and expensive.

A thicker isolator such as 2mm alumina can reduce the capacitance by a factor of 10, but in this application, heatsink paste would be needed, and thermal resistance would be significantly degraded. The first rule of good EMI practice is to eliminate noise generators at source when possible; here it is easy, a transistor with the cooling tab connected to source would eliminate the switched voltage charge injection into the heatsink. TO-247 packed GaN transistors with source connected cooling are available from multiple vendors with source tabs, Nexperia kindly sampled the GaN-063-650W.

Modifications for the GaN transistor

The first thing to note is the GaN has a different pinout to a standard TO-247. The standard MOSFET has, the drain in the middle; the GaN has the source as the centre pin. To replace the MOSFET with the GaN transistor; the GaN legs had to be bent, with the drain and source being effectively swapped. PTFE sleeving was used to guarantee isolation. Reforming the leads meant that the source on the GaN is longer than usual and has more inductance; which could create problems with switching and possible oscillation at high currents. This isn't ideal, but does permit a quick first look without a redesign of the board.

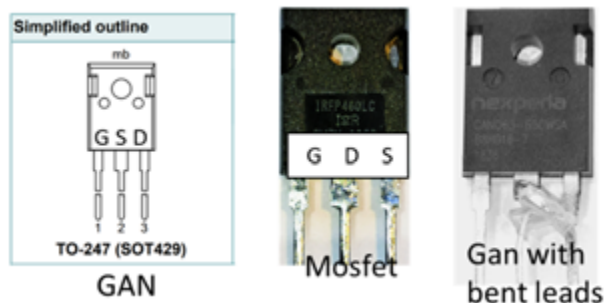


Figure 3: Reforming Gan legs

The GaN gate charge with 15nC is about a tenth of a similar MOSFET, so the gate resistor was increased to 18 Ω it also meant that the extra driver stage could be removed and the transistor could be driven directly from the PFC controller.

Measurements

Figure 4 shows comparable drain-source switching waveforms. The first surprise was clean switching waveforms, despite the bent leads. Turn-off Switching speeds (dV/dt) are similar, but the GaN does not have the initial slow rise time at the beginning of turn-off. The short delay between the gate going low and switching is a benefit of the much much smaller output capacitance at $V_{ds} < 50V$. The GaN turn-on is somewhat faster, with 40V/nS it is about twice as fast as the MOSFET, ringing at turn-off is similar. There is more ringing at turn-on which not too surprising considering how the transistor is mounted with extended reformed leads with a very long source lead.

EMI plots in figure 5 show clearly, the benefit of the source connected tab. The whole spectrum looks cleaner, with about 10dB lower emissions at 170kHz. Tests showed the 170kHz emissions could be further

reduced by adding a larger x capacitor, whereas with the MOSFET larger Ycaps and Xcaps would be needed. The MOSFET has a rise time of 20nS, compared to the GaN 10nS so that the GaN noise spectrum would have the double cut off frequency, but more important is the virtual elimination of the capacitance of the switched drain to the heatsink. With the injected currents in the chassis eliminated by using the GaN; we expected the chassis to be quiet. Further investigation revealed the inductance of the SiC diode cathode lead, was now the primary noise injector into the chassis. The switched current in the cathode lead inductance, induce a voltage on the tab. This voltage is capacitively coupled to the heatsink and injects current into the chassis. As there is no large voltage here, a small snubber between the diode lead and elco removed most of the noise with minimal cost and power loss. Typical EMC, remove one source of noise only to then discover more.

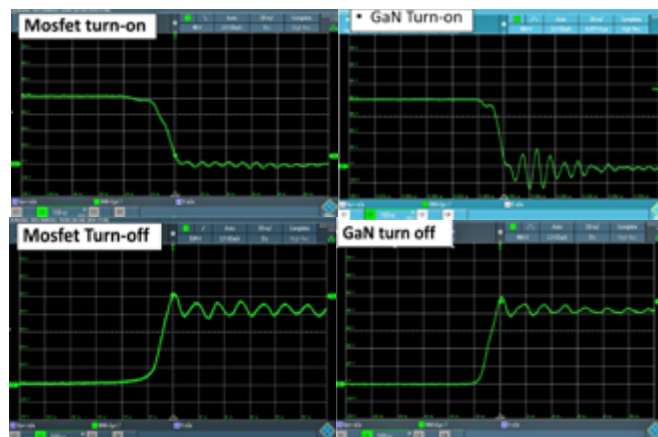


Figure 4: Switching Waveform Comparison

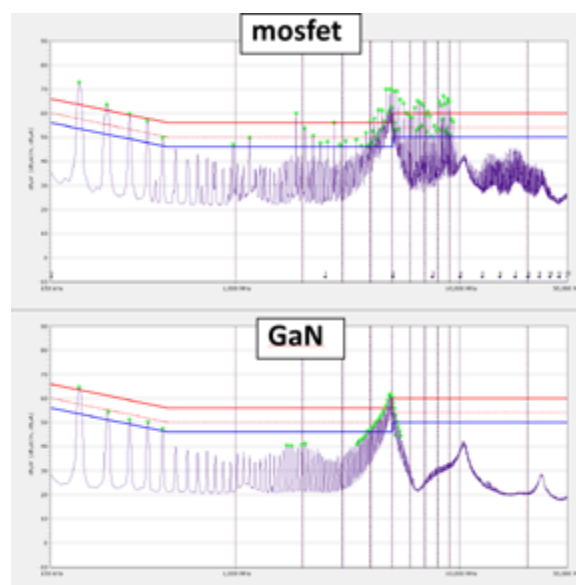


Figure 5: EMI Measurement Mosfet and GaN

Conclusion

Using the source tabbed transistor eliminated a significant source of EMI at its origin. I was surprised by how well the GaN performed despite having the long bent leads. The pinout with the source centre pin TO-247 will allow a much better layout than the current drain tabbed transistor, with probably more EMI improvements and lower losses.

Nigel.Springett@springburo.de

Innovative Manufacturing Approach Reduces Costs and Optimizes Electrification Time to Market

Manufacturers looking to enter or expand their electrification business often find themselves balancing key production requirements with the unpredictability of an emerging market where best-practice standards are still evolving. To meet these challenges, Comau is rethinking electrical motor and transmission assembly by fully integrating design validation, resin verification, rotor preparation/winding, and multi-model manufacturing flexibility as part of a functional, efficient and versatile operational philosophy.

*By Ermanno Faccin, Head of Powertrain & Electrical Drive Unit
- Assembly & Test, Comau*

Backed by pioneering competencies in electrification and a 360° understanding of automotive manufacturing, the Italian automation leader has developed a strategic and straightforward approach to rotor and stator assembly that optimizes cycle times, eliminates resin compatibility issues, and can be easily integrated within pre-existing production lines.

The method starts with a fully integrated design phase. Often done in simultaneous engineering with the client, the team looks at the performance and product considerations before identifying the optimal combination of processes and technologies for the specific nature of the project. Looking at the electrical motor architecture evolution, many automakers in recent years have been investing in permanent magnet rotors and hairpin stators. At the same time, wound rotors continue to command an important share of the market both due to their performance and because the cost of retooling an existing line is often significantly less than investing in a new line. Another advantage of the wound rotor is its efficiency. Wound rotors enable better energy management due to the fact the magnetic field can be modulated by electronics management, whereas the permanent magnet rotor (PM/IPM) has a fixed magnetic field.

When building a slip-ring rotor there are several process considerations that must be evaluated carefully based on factors such as the motor design and projected production volumes. One of the key decision points involves the electric winding and impregnation phases, which directly affect the performance and life cycle of the assembled e-motor. Here, the choice of spindle, needle or flyer winding depends largely on comparing the wire management process, winding quality and the height and width of the rotor teeth. The first difference lies in the wire management process. With spindle winding the wire passes straight through a guide tube into the winding chamber and onto the outer flanges, which protect the wire from the side teeth, before

reaching the layering flanges. The direct nature of this process means that the wire tensioner can manage up to 90% of the wire tension. Needle winding, on the other hand, requires that the wire first pass through the needle head, where it is bent 90°. It then enters the wire guide tube where after another 90° bend it passes into the winding chamber. Because the tension control is offset by the needle head, the tensioner only manages about 60% of the final wire tension.



Figure 1: Comau is rethinking electrical motor and transmission assembly

Indeed, the wire tension, wire angle and ratio between the height and width of the teeth are three factors that can determine the uniformity of each coil layer. When comparing winding technologies, spindle winding tends to produce a more even wire distribution than needle winding due to its straight-line feed process. This is further aided by the good tension management and high reactivity of the tensioner. As the needle wound wire comes out of the wire guide at 90° and is already subject to stress, there is a greater possibility for the winding to become concave. At the same time, the tensioner is not fully able to control the final wire tension and there is a limited possibility to quickly

pull the wire back during the different winding phases. These factors contribute to the risk of convex winding. Increasing the wire tension can reduce the distortion but will also increase the final Ohmic value.

Another consideration is the rotor's mechanical design. Spindle and needle technologies require slightly different spacing parameters, which in some cases may favor or eliminate one of the two options. In spindle winding, the space between the teeth needs to accommodate both the layering flange and the wire itself (approximately 2.5 mm). The space required for needle winding is determined by the thickness of the wire guide tube. Generally speaking, this means there will be between 1.4 mm up to 3.6 mm of space between the teeth.

Comau's experience in electrification gives us a unique ability to design efficient, high-volume, automated assembly lines for the entire e-motor assembly process. We do this by comparing different techniques, analyzing performance requirements and integrating different proprietary technology platforms within a fully automated manufacturing process. Furthermore, as a single-source provider, we harmonize the collaboration between specialists, technology companies and systems integrators to optimize the entire program rollout. The end result of our turn-key engineering offer is the assurance that production can be done in the most effective way possible, with reduced costs, maximum productivity and faster time to market.



About the Author:

Ermanno Faccin leads the proposal team to support Comau customer's needs by providing efficient manufacturing solutions in traditional and innovative industrial sectors as Head of Powertrain & Electrical Drive Unit - Assembly & Test. After graduating with a degree in Mechanical Engineering at Turin Polytechnic in 1995, with a specialization in industrial automation and innovative manufacturing systems, he

interned with Comau in a European program dedicated to high-speed machining process optimization in the automotive industry.

After dedicating fifteen years to project execution with the main car builder in EMEA, APAC, North America and LATAM, he embraced the leadership of the standard product development dedicated to the flexible, modular, and scalable assembly systems applied in powertrain environments.

With electrification development booming in the automotive business, he has been leading the engineering proposal team from Europe for five years. In this role, he is responsible for offering Comau's customers the performance, quality, and competitiveness relevant to electrical powertrain and battery assembly systems.

www.comau.com

emv
...goes digital

Digital, 23 – 25 March 2021

Get a unique market overview and new impulses for your daily work: Exchange with experts at the European meeting point for electromagnetic compatibility.

Discover more: e-emv.com

FET for 48 V Synchronous Rectification

Efficient Power Conversion advances the performance capability while lowering the cost of off-the-shelf gallium nitride transistors with the introduction of the EPC2059 (6.8 m Ω , 170 V) eGaN FET. This device is the latest in a family of 100 V – 200 V solutions suitable for a wide-range of power levels and price points. They are designed to meet the increasing demands of 48 V – 56 V server and data center



products as well as an array of consumer power supply applications for high end computing, including gaming PCs, LCD/LED TVs, and LED lighting. The EPC2059 is ideal for DC-DC secondary-side synchronous rectification in AC/DC adaptors, fast chargers, and power supplies with power ranges between 100 W and 6 kW. The performance advantage of gallium nitride devices helps designers achieve the demanding efficiency requirements for 80 Plus Titanium power supplies, while providing smaller, faster, cooler, and lighter systems with lower system costs than currently available solutions. According to Alex Lidow, EPC's co-founder and CEO, "There are very significant performance advantages gained from using GaN in the secondary-side synchronous rectification socket of AC/DC adaptors. In a 400 V to 48 V conversion, switching at 1 MHz, GaN has shown to have one-sixth the losses and run 10 degrees cooler than a silicon MOSFET with equivalent on resistance. This enables designers to meet the latest stringent energy efficiency standards for high-end computing, where growth is exploding for multiple applications, such as artificial intelligence (AI), cloud computing, and high-end gaming systems."

www.epc-co.com

Automotive-Compliant Synchronous Buck Converters

Diodes Incorporated has announced two highly integrated synchronous buck converters that simplify circuit design in automotive power systems with its Power Good output and its innovative EMI mitigation for noise-sensitive applications. The AP63356Q and AP63357Q are 3.5A converters with an input voltage range of 3.8V to 32V. Leveraging peak current mode control as well as high-side and low-side

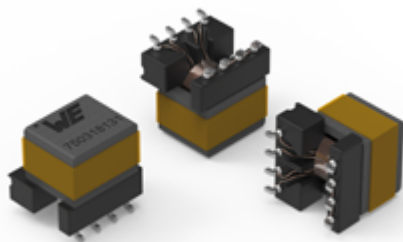


power MOSFETs on-chip, the converters minimize external components to reduce bill of materials (BOM) costs and board size. Both devices have a Power Good indicator with an internal 5M Ω pull-up resistor useful for power sequencing. To further aid sequencing, their enable pin has accurate voltage thresholds, which allows adjustment of the input voltage device power-on and undervoltage lockout (UVLO). The high-voltage capability of the EN pin allows direct connection to VIN to simplify the auto-start of the device. When disabled, the converter draws only 0.6 μ A shutdown current typical. Their proprietary gate-driver scheme ensures clean switching transitions while preventing switch-node ringing to minimize high-frequency radiated noise. Frequency spread spectrum (FSS) contributes further to quiet performance by dispersing switching-noise energy. The AP63356Q operates continuously in PWM mode at the nominal 450kHz switching frequency for all loads. The AP63357Q changes to PFM mode at light loads, keeping efficiency as high as 86% at 5mA load and drawing quiescent current of just 22 μ A under no load.

www.diodes.com

Part of a High-Performance Power Supply

Würth Elektronik presents its WE-AGDT transformers for SiC MOSFET gate drivers. It makes a new SMT assembly transformer available, which, at the same time, is part of a power supply solution developed by Würth Elektronik for demanding gate control of SiC MOSFETs. The innovative WE-AGDT is a compact transformer in an EP7 package. It features a wide input voltage range from 9 to 36 V, a high saturation current of 4.5 A, as well as very low leakage inductance, and a very low capacitance of 6.8 pF between the windings. This gives rise to high common-mode transient immunity (CMTI) of the gate driver system.



The WE-AGDT series comprises six transformers, each optimized for its respective reference design. Thanks to their two separate secondary windings, they allow both

bipolar (+15 V, -4 V) and unipolar (+15 V to +20 V, 0 V) output voltages. The input voltage of 9 to 36 V achieves a maximum output power of 3 to 6 W. WE-AGDT transformers are optimized for SiC applications, but are also suitable for optimally controlling IGBT and power MOSFETs, and, given a suitable DC-DC converter, even for high-voltage GaN FETs. Würth Elektronik's reference design for a compact, galvanically isolated DC-DC converter for SiC MOSFET gate drivers is available at www.we-online.com/rd001.

www.we-online.com/agdt

Automotive Primary DC/DC Converters

ROHM has developed a lineup of twelve automotive primary DC/DC converters. The BD9P series are optimized for ADAS (Advanced Driver Assistance System) sensors, cameras, and radars, along with car infotainment and instrument clusters. The need for fast response to provide stable operation and higher power conversion efficiency are crucial, which have been difficult to meet with conventional power supply ICs. The product adopting original advanced power supply technology, Nano Pulse Control™, enables high speed operation at 2.2MHz that will not interfere with the AM radio band (1.84MHz max.) while achieving high step-down ratio. It is an optimum technology for automotive applications. The BD9P series ensures stable operation during battery input voltage fluctuation, reducing output overshoot to less than 1/10th of that of conventional products. This eliminates the need for additional output capacitors typically required as countermeasure against overshoot. Additionally, adopting a new control method makes it possible to achieve both high efficiency and fast response (which typically represent a tradeoff). Not only does this provide a 92% power conversion efficiency at heavy loads (at 1A output current), but 85% efficiency at light loads (1mA) as well, ensuring leading-class efficiency across the entire load range. As a result, low power consumption is enabled both when driving and when the engine is stopped (standby current can be reduced).



Furthermore, combining the new product with the BD9S series of secondary DC/DC converters connected to the subsequent stage leads engineers to faster design of more efficient automotive power supply circuits.

www.rohm.com

www.bodospower.com



embeddedworld2021
Exhibition & Conference

DIGITAL

**EMBEDDED.
INTELLIGENT.
SYSTEMS.**

JOIN THE DIGITAL EVENT!

1 – 5.3.2021

Get your ticket now!
embedded-world.com/tickets



Media partners

Markt & Technik
THE LEADING MAGAZINE FOR ELECTRONICS

Elektronik
Magazin für Elektronik

SmarterWorld
Solutions for a Smarter World

DESIGN & ELEKTRONIK
KNOW-HOW FOR ENTWICKLER

Elektronik automotive

Computer's AUTOMATION
Partnerium der Automobilwirtschaft

• **medical-design**

elektroniknet.de

NÜRNBERG MESSE

100V High-Speed, Half Bridge Evaluation Board

GaN Systems announced a 100V High-Speed, Half-Bridge Evaluation Board (GS-EVB-HB-61008P-ON) in collaboration with ON Semiconductor. Available now through distribution partners, this solution is developed for existing and new PCB designs and allows power electronics designers to easily evaluate GaN for growing 48V market applications, including non-isolated step-down converters, non-isolated step-up converters, and half-bridge and full-bridge converters. The evaluation board includes an OnSemi NCP51810 GaN driver and two GaN Systems GS61008P E-mode GaN power transistors connected in a high-side, low-side configuration and all necessary drive circuitry. It provides the utmost flexibility of GaN transistor and driver combinations and can be applied in any topology that requires the use of a high-side/low-side FET combination. When connected into an existing power supply, it can replace HS/LS drives and MOSFETs. The evaluation board also offers configurable dead-time control and driver enable/disable functions.

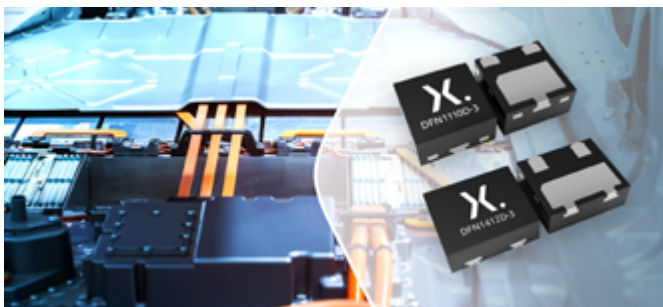


One of the major benefits is the evaluation board's small size and simplified yet robust design. Several pins are available to probe the circuit. HS and LS gate drives, as well as SWN are accessible. Additional benefits include fast propagation delay of 50 ns max, increased efficiency and allows paralleling, and control of rise and fall time for EMI tuning.

www.gan-systems.com

AEC-Q101-Qualified CAN-FD Protection Diodes

Nexperia has announced leadless ESD protection devices for CAN-FD applications. Devices are available in leadless packages with side-wettable flanks that enable AOI tools to be used. Fully AEC-Q101-qualified, the PESD2CANFDx series parts also offer industry-leading



ESD and RF performance, and save PCB space. Nexperia offers silicon-based ESD protection for the CAN-FD bus in both leaded and leadless packages. The DFN1412D-3 and DFN1110D-3 leadless

DFN packages with side-wettable flanks occupy 80% less PCB space than traditional SOT23 and SOT323 packages. Despite this, products assembled in this package feature improved thermal behaviour due to a larger internal lead frame that includes a heatsink and thermal pad. PESD2CANFDx diodes are also very ESD robust delivering excellent system level protection performance. This is because the parts have industry's lowest clamping voltages of only 33 V at IPP = 1 A and low dynamic resistance of 0.7 Ω . Nexperia ESD protection devices also offer very good RF switching parameters featuring a mixed mode insertion loss of just +20 dB at 300 MHz, leading to excellent signal integrity. Commented Nexperia's product manager Lukas Droemer: "CAN-FD is an important bus in automotive in-vehicle networks but devices must be protected against ESD. Another essential requirement for automotive applications is the ability to use AOI. Our new devices in leadless packages meet both these requirements, providing a high-performance alternative to leaded SMD packages."

www.nexperia.com

IC Featuring Internal Self-Discharge Monitoring and Protection

The MAX17320 fuel-gauge and protection circuit from Maxim Integrated Products extends run-time on multi-cell battery-powered products while also monitoring against self-discharge hazards. The MAX17320 is a pack-side fuel gauge and protector IC for 2 to 4 series Lithium-ion (Li+) cells (2S-4S) and is part of a family of ICs equipped with Maxim Integrated's patented ModelGauge™ m5 EZ algorithm that delivers 40 percent more accurate state-of-charge (SOC) readings than competitive offerings, eliminating the need for battery characterization for most common Li+ cells. This fuel gauge also offers the industry's lowest quiescent current (IQ), which is 85 percent lower than the nearest competitor and features SHA-256 authentication to safeguard systems from counterfeit batteries.

For hand-held devices with 2S-4S Li+ batteries in the computing, internet of things (IoT), power tool, consumer, healthcare and mobile device categories, ensuring customer safety is top of mind for designers. Damaged or defective batteries may develop an internal cell leakage which can progressively get worse and can result in dangerous outcomes, including fire or explosion. This can endanger consumers and tarnish brand value for manufacturers. Stringent factory screening



may prevent leaky cells from getting shipped out of the factory. However, until now there were no solutions for detecting self-discharge that develops during normal usage of the battery. The MAX17320 warns the system and disables a leaky battery before a potentially hazardous outcome.

www.maximintegrated.com

DC-DC Converters for USB-PD Applications

Silanna Semiconductor announced the launch of wide voltage, high frequency point of load converters targeting USB-PD applications. Silanna Semiconductor focuses on ultimate Power Management challenges with best in class power density and efficiency performance that delights customers with unprecedented BoM savings. SZPL3102A/3103A family of two DC-DC converters (Buck Regulators) operate up to 2MHz. Delivering industry leading wide input and

output range converters that support up to 27VDC input in a tiny 3mm X 3mm QFN. Tim Wilhelm, Director of Marketing, explained, "Higher switching frequency means a smaller, lower cost output filter that has delighted the clients we have sampled. The SZPL3102/3103 have ground-breaking efficiencies in the smallest size and weight designs. Our support tools give customers the flexibility and confidence to quickly increase the performance efficiency which ultimately increases the power density in their designs approaching 12% of the volume required by low frequency competitive solutions. The SZPL3102/3103 significantly reduce BOM cost, design cycles and time to market." The SZPL3102A and SZPL3103A have unique features that optimize their performance in USB port power supply applications. Extremely low operating power dissipation enables very low no-load power that is an important specification for regulatory certification. Furthermore, the SZPL3102A contains a momentary internal feedback path that allows for clean and well controlled start-up operation until external USB-PD controllers can bias themselves and take over control of the output voltage.



www.powerdensity.com

Fast Switching 600V Super Junction MOSFETs

Alpha and Omega Semiconductor announced the release of a Fast Switching 600V α MOS5™ Super Junction MOSFETs in SMD-type TOLL Package. α MOS5 is AOS's latest generation of high voltage MOSFET, designed to meet the high efficiency and high-density needs for Quick Charger, Adapter, PC Power, Server, Industrial Power, Telecom, and Hyperscale Datacenter applications.

The α MOS5 TOLL product's footprint is only 115mm², which is 23% smaller than that of D2PAK. Its package thickness is 2.3mm, an almost 50% height reduction versus D2PAK. The reduced package inductance and parasitics of the TOLL package enable power designs to reach the next level of switching efficiency, EMI performance, and ease-of-use. The first Fast Switching α MOS5 TOLL product will be available as AOTL125A60, a 600V device of 125mOhm. Upcoming α MOS5 TOLL products will provide a much wider range of Rds(on), covering applications from 200W to 3kW. Furthermore, α MOS5 TOLL provides a current capability of up to 100A in a 125mohm device, supporting today's most demanding Server PFC and PV Inverter applications, which require both high current rating and small form factor. The Automated Optical Inspection (AOI) Capability and Enhanced Solder Contact Area of α MOS5 TOLL also help improve the system and board-level reliability of power supplies that need to serve long life cycles. Additionally, α MOS5 High Voltage TOLL package features Kelvin Source connection, which significantly improves switching performance by reducing switch-on loss through separate power and drive sources.

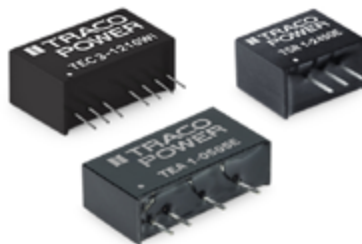


www.aosmd.com

Campaign for "Low-Cost" DC-DC Converter

The TSR-E, TEA, TBA and TEC series are available from 1 to 3 watts covering 12 product families. They all focus on a simple and effective design approach which is unique to those Traco Power Products.

By innovative engineering we have come up with an electrical design which minimises component and labour costs. Key focus of those designs was to maximise the amount of automation of the manufacturing process. With this innovative product design, we optimised the automation of the manufacturing process to the maximum. This enabled us to launch cost and quality optimised, low



power dc-dc converters which are ideal for your high volume IoT projects. Florian Haas, Director of Global Marketing and Product Management states more precisely: "We have listened to the market and are pleased

to launch the campaign of our new low-cost DC-DC converters. With the TSR 1E (non-isolated, regulated), TEA/TBA (isolated, unregulated) and TEC 2/3 (isolated, regulated) series models, we give designers a choice of high quality, cost-optimised DC-DC converters from 1-3 watts. Unlike our competitors, we focus in the campaign not only the price reduction, but also HOW we can achieve these low manufacturing costs and what benefits these products bring to the customer."

www.tracopower.com

Flat Aluminum Electrolytic Capacitors

Cornell Dubilier Electronics has expanded its line of high performance flat electrolytic capacitors with the NHR Series. Able to withstand operating temperatures from -55°C to 150°C , NHR capacitors are con-



CDE CORNELL DUBILIER NHR Series 150°C and 80g Vibration Flat Aluminum Electrolytic Capacitors
Landing page: <https://cde.com/new-product/nhr>
Data Sheet: <https://cde.com/resources/catalogs/nhr.pdf>

structed with rectangular stainless-steel cases and laser-welded covers that prevent dry-out. These capacitors have a 3,000-hour life at full-rated conditions and withstand up to 80g vibration to meet the most demanding military, aerospace, industrial, and down-hole applications. Type NHR is a spin-off of the company's Flatpack series that has been proven in military and aerospace applications for nearly 30 years. "Our NHR Flatpack technology offers exceedingly long life at high temperature for critical applications that previously have been the domain of wet-tantalum capacitors," said Mario DiPietro, Product Manager for Cornell Dubilier. "Their high-capacitance density at high voltage and temperature solves many of the problems faced by engineers designing circuits for extreme environments," continued DiPietro. The company claims it has had considerable success in helping its customers replace large series-parallel banks of wet tantalum capacitors with fewer components, saving them valuable space, weight and cost. Components within the NHR series are available from 75 Vdc through 300 Vdc with capacitance values ranging from 60 μF to 960 μF . There are four case lengths available in 0.5" increments from 1.5" to 3.0". All cases measure 0.5" thin by 1.0" wide.

www.cde.com

RF Switch with 4 Channels and 25W Power Handling

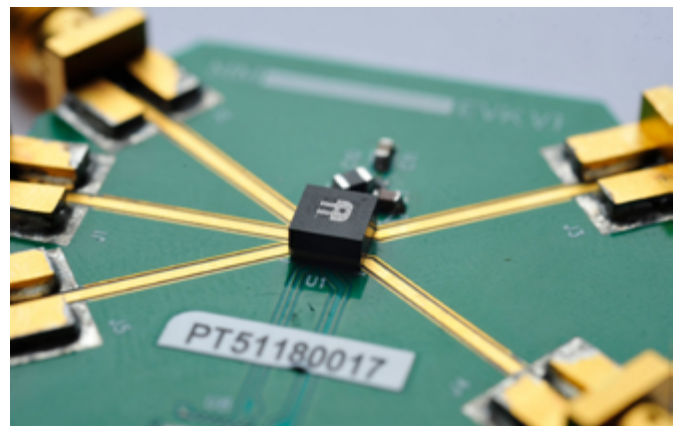
Menlo Microsystems announced the production release of the MM5130, the first high performance RF switch manufactured with their proprietary Ideal Switch™ technology.

The MM5130 is designed to handle 25W with ultra-low losses, in a miniaturized wafer-level chip-scale-package (WL-CSP). Historically, this level of performance has been reserved for large RF mechanical relays, which have major drawbacks. With its Ideal Switch™ technology, Menlo Micro has eliminated the compromises that engineers have had to make when selecting between RF mechanical relays and solid-state switches. The MM5130 offers the power handling and RF performance of an electromechanical relay (compared below), with the size, reliability, and speed of a solid-state switch.

These improvements make the MM5130 switch a very attractive solution for a multitude of applications including low loss switched filter banks, tunable filters, step attenuators, and even beam steering antennas for a variety of radio architectures in both commercial and military communications networks. The high-channel density and low losses also make the MM5130 ideal for ultra-compact switch matrices for test and measurement applications.

"We are very excited to announce that the MM5130, and more importantly our Ideal Switch™ manufacturing line, is ready for production," said Menlo Micro co-founder and SVP Marketing, Chris Giovanniello.

"With this milestone, companies will begin to realize our vision of mas-



sive reductions in the size, weight, and power across a wide variety of RF subsystems. With over 30 customer design-ins to date for the MM5130 in 5G, aerospace & defense, and test & measurement applications, the number of companies taking advantage of the unique performance benefits of the Ideal Switch™ continues to grow."

www.menlomicro.com

Advertising Index

Advanced Conversion	17	Fuji Electric Europe	11	PCIM Europe	30
APEC	C3	GvA	C1	Plexim	13
Cornell Dubilier	23	Hitachi	9	ROHM	7
Electronic Concepts	1	Hitachi ABB Power Grids	35	Sirio Elettronica	27
embedded world	45	LEM	5	UnitedSiC	19
emv	43	Mitsubishi Electric	31	Vincotech	15
EPC	C4	MUECAP	37	Würth Elektronik eiSos	3

The Premier Global Event
in Power Electronics™

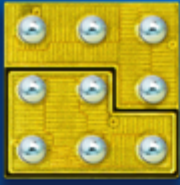
APEC[®]
2021

PHOENIX

JUNE 9-12TH, 2021



EPC2106 - 100 V eGaN[®]
Half Bridge



**70 m Ω , 1.7 A,
18 A_{pulsedr} 1.8 mm²**



AUTOMOTIVE



MOBILE



ROBOTICS



SERVER



SOLAR



SPACE



TELECOM

GaN-Based Motor Control

Smaller • Lighter • Silent Operation

eGaN[®] FETs and ICs provide the **small size, light weight, and quiet operation** that brushless DC (BLDC) motors require for applications such as robotics, automation, and drones.



Note:

Scan QR code to learn how to reduce audible noise for quiet motor drive operation.

<https://bit.ly/Bodo0121>



EFFICIENT POWER CONVERSION

epc-co.com